MicroRNAs, senescence et vieillissement

Dr Brondello Jean-Marc, INSERM U1183
Cellules souches et pathologies osteo-articulaires
St Eloi,IRMB, Montpellier
Jean-marc.brondello@inserm.fr

La révolution autour des microARNs

De la petunias aux patients

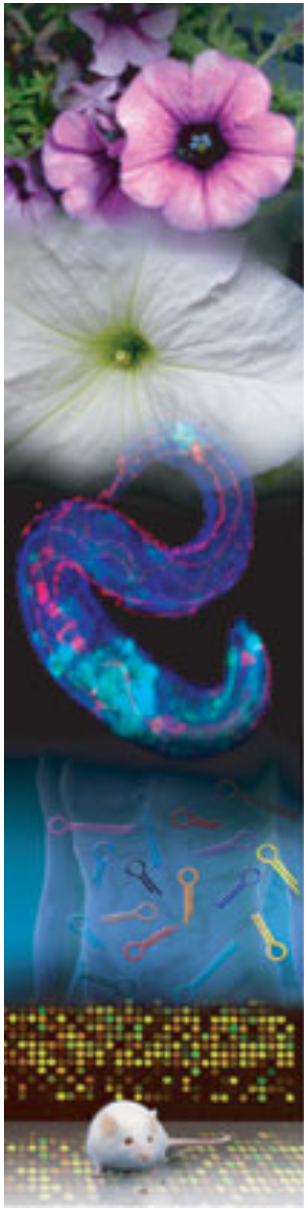

1990

Researchers insert extra RNA into petunias to make them deeper purple but got pure white, suggesting the existence of an unknown gene-silencing mechanism (Napoli et al)

1993

Discovery of lin-4 microRNA, which guides development of the *C. elegans* worm (Ambros et al)

1998

RNA interference is discovered in *C. elegans*, solving the petunia puzzle

2000

The presence of microRNAs in human cells is established

2001

Hundreds of new microRNAs are discovered in animals and plants

2006

Nobel Prize: **Andrew Z. Fire, Craig C. Mello**

2008

1st clinical trial of microRNA-based therapeutic drug: antago-miR122 in liver infection by HCV

1990

1995

2000

2005

2010

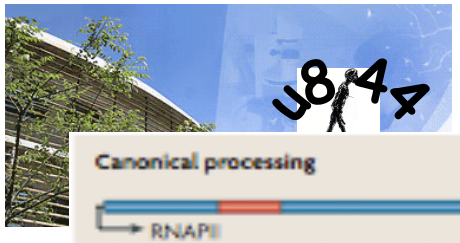

Processing des miRs

15% des Mirs sont en cluster

60% des Mirs ont leur propre promoteur

25% sont des mitrons

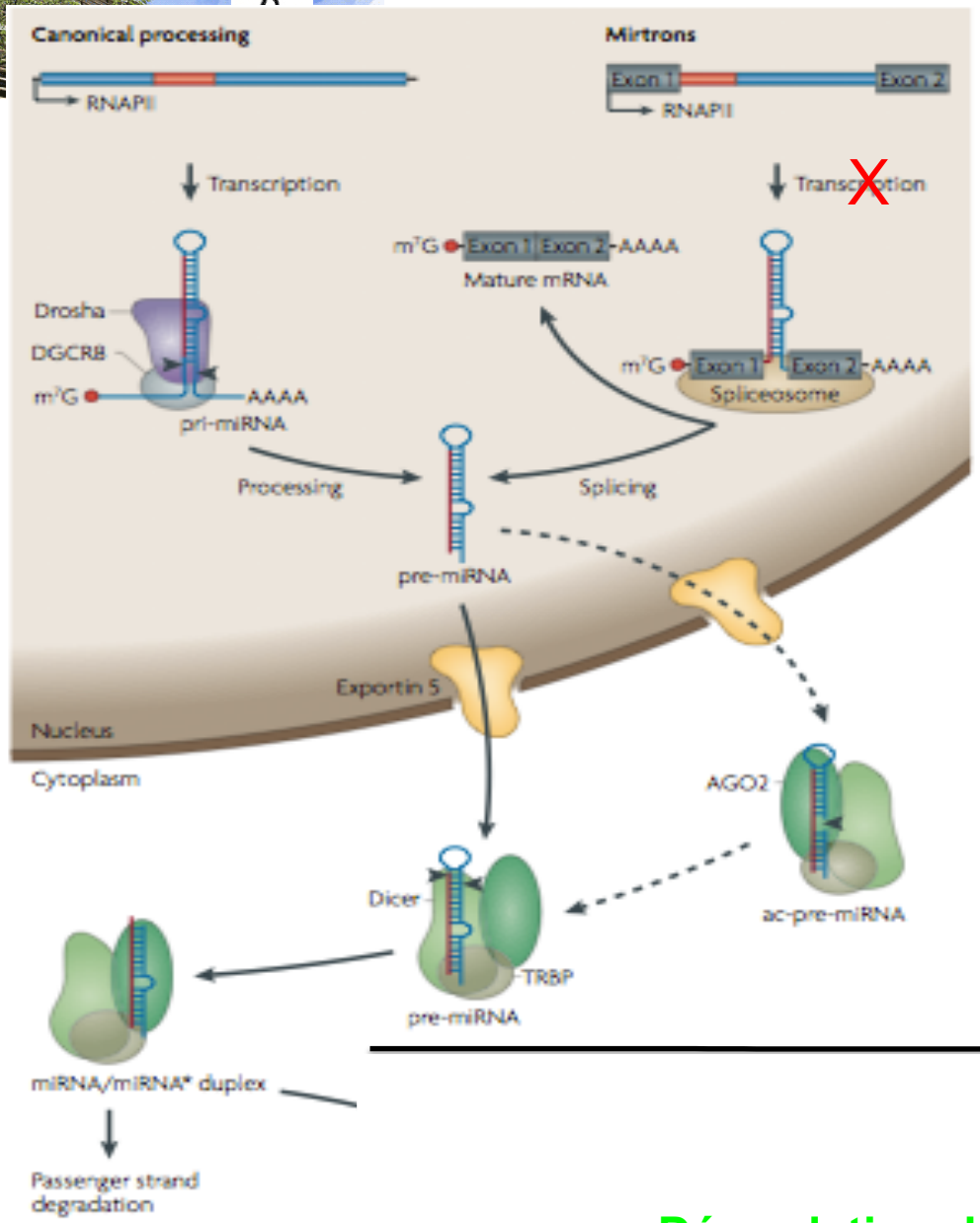

Répression de la traduction

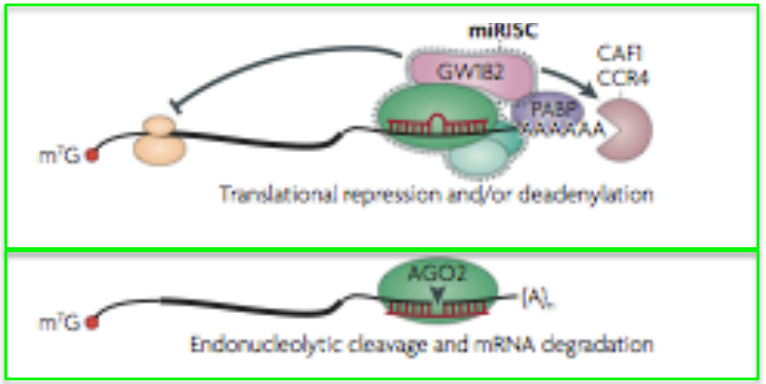

Dégradation des ARNm

Krol et al, *Nat. Review genetic*, 2010

Dans le génome on retrouverait environ

1-1400 miRs

2-Entre 25 et 50% des gènes seraient régulés par des Mirs

3-Les Mirs induisent une dégradation d’ ARNm dans 20-30% des cas

4-Dans le reste des cas, les miRs bloquent la traduction

Pairing microRNA/mRNA

Ex:

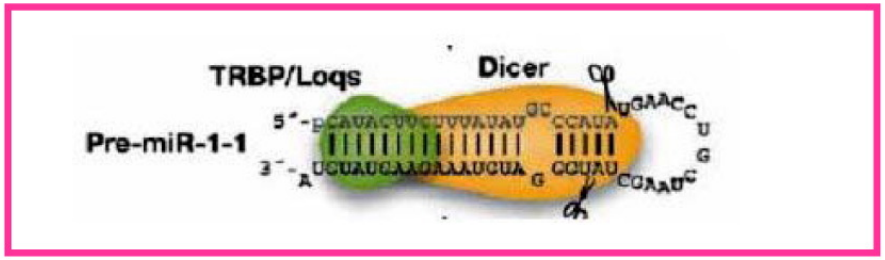

3’UTR mRNA target sequence

miRNA seed sequence
(positions 2–8)

Le pairing en 3’UTR a permis le développement de logiciels de prédictions des cibles des Mirs

Ex: targetscan/miranda/RNA22/Diana etc…..

Conséquences:

Les publications récentes se basent sur les prédictions de
plusieurs de ces logiciels

Mais……

Vol 460|23 July 2009|doi:10.1038/nature08170 nature

ARTICLES

Argonaute HITS-CLIP decodes microRNA–mRNA interaction maps

Sung Wook Chi[1], Julie B. Zang[1], Aldo Mele[1] & Robert B. Darnell[1]

MicroRNAs (miRNAs) have critical roles in the regulation of gene expression; however, as miRNA activity requires base pairing with only 6–8 nucleotides of messenger RNA, predicting target mRNAs is a major challenge. Recently, high-throughput sequencing of RNAs isolated by crosslinking immunoprecipitation (HITS-CLIP) has identified functional protein–RNA interaction sites. Here we use HITS-CLIP to covalently crosslink native argonaute (Ago, also called Eif2c) protein–RNA complexes in mouse brain. This produced two simultaneous data sets—Ago–miRNA and Ago–mRNA binding sites—that were combined with bioinformatic analysis to identify interaction sites between miRNA and target mRNA. We validated genome-wide interaction maps for miR-124, and generated additional maps for the 20 most abundant miRNAs present in P13 mouse brain. Ago HITS-CLIP provides a general platform for exploring the specificity and range of miRNA action *in vivo*, and identifies precise sequences for targeting clinically relevant miRNA–mRNA interactions.

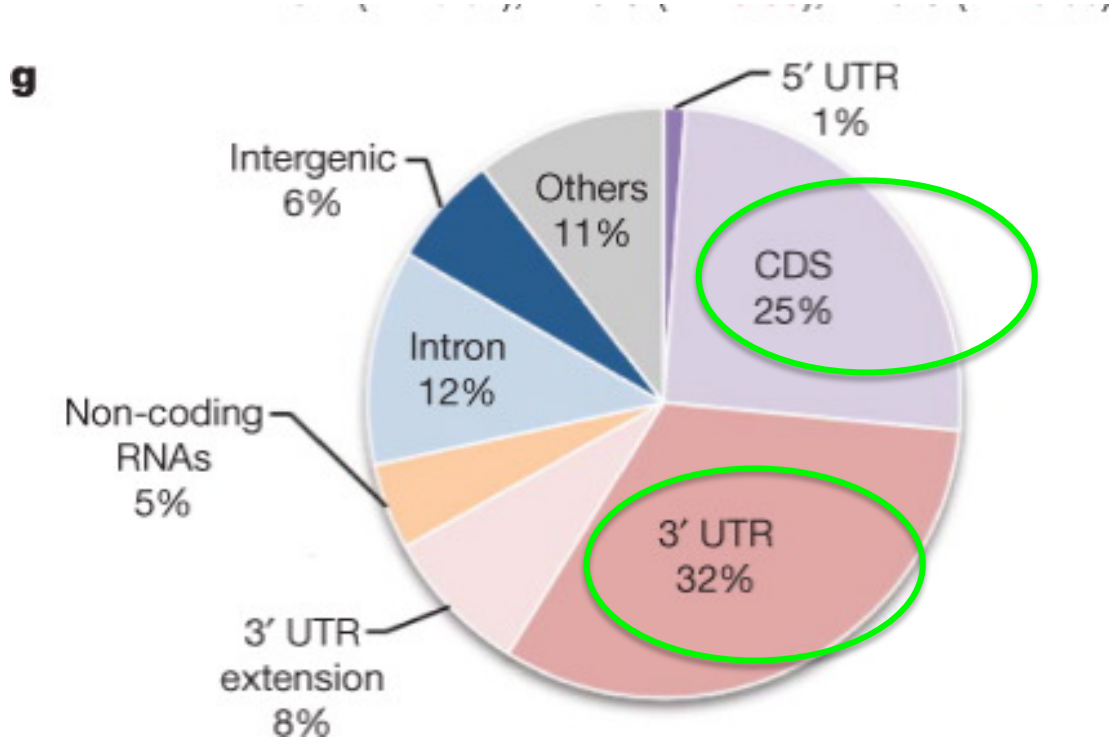

Les dogmes concernant les cibles des miRs en 3’UTR sont à prendre avec précaution

Conclusions I

- Domaine en évolution permanente
- Interrogation sur les analyses in silico d'identification de cibles
- Possible interférence d'un miR sur plusieurs voies de signalisation ou de mécanismes cellulaires
- Rôle des SNP sur les miRs (ou leurs cibles), permet d'expliquer leur rôle dans plusieurs populations à risque à développer une pathologie donnée

Maintien de la stabilité génétique

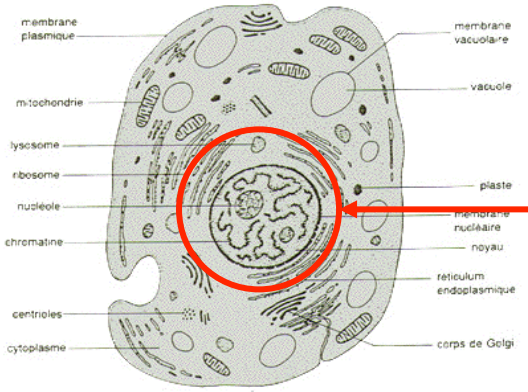

Métabolisme de l'ADN

Mécanismes anti-vieillissement
Ou mécanismes de longévité

Vieillissement cellulaire, perte de fonctions

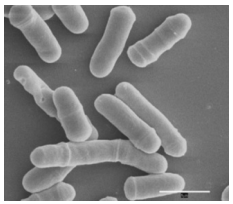


Pathologies de vieillissement prématuré:

- **Werner syndrome**
- **ataxia telegenectasia**
- **Dyskerotosis congenita**

induit la dégénérescence des tissus,

Apparition de pathologies liées à l'âge
(arthérosclérose, arthrose, hyperplasie de la prostate, Ulcération, peau, immunité, cancer)

Vieillissement de l'organisme

Environmental Factors
(mechanical stress Cytokines, Uvs, oncogene)

intrinsec Factors
(oxidative stress- DNA repair defects, erosion des téloméres)

Cellular Senescence

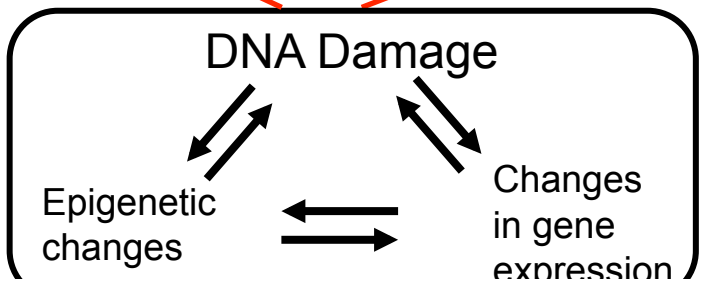

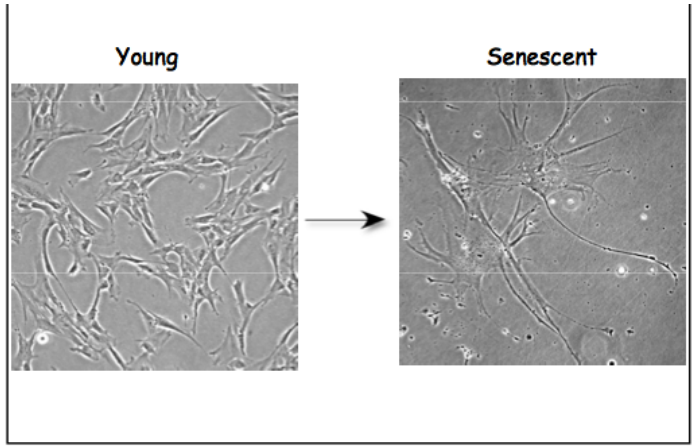

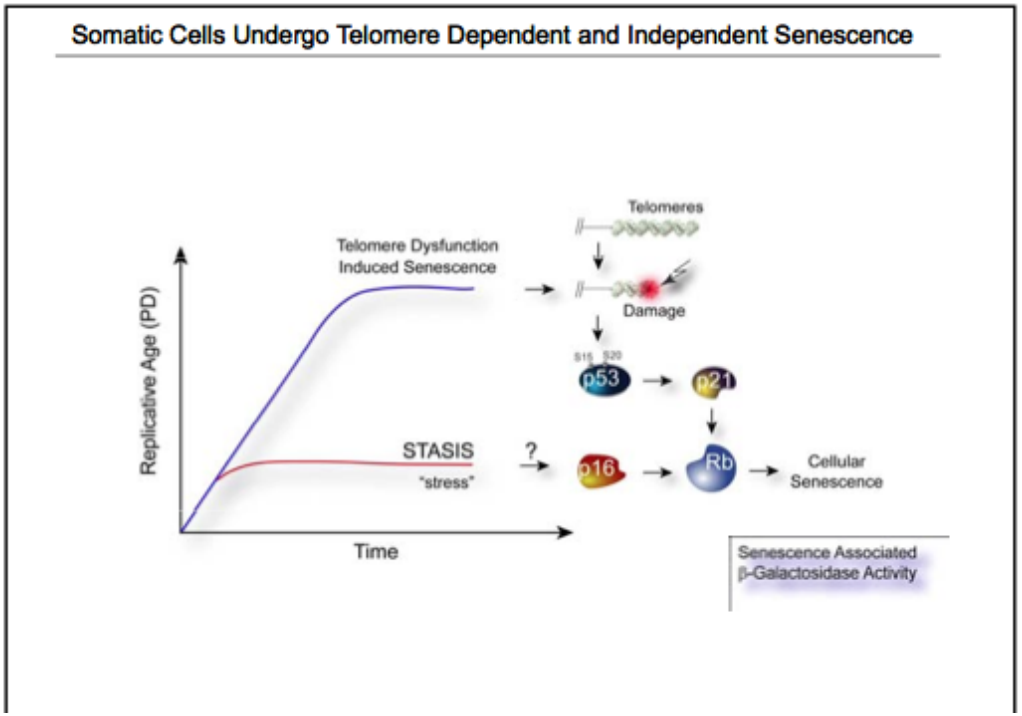

Adapted from Brunet A. et al, Nature 2007

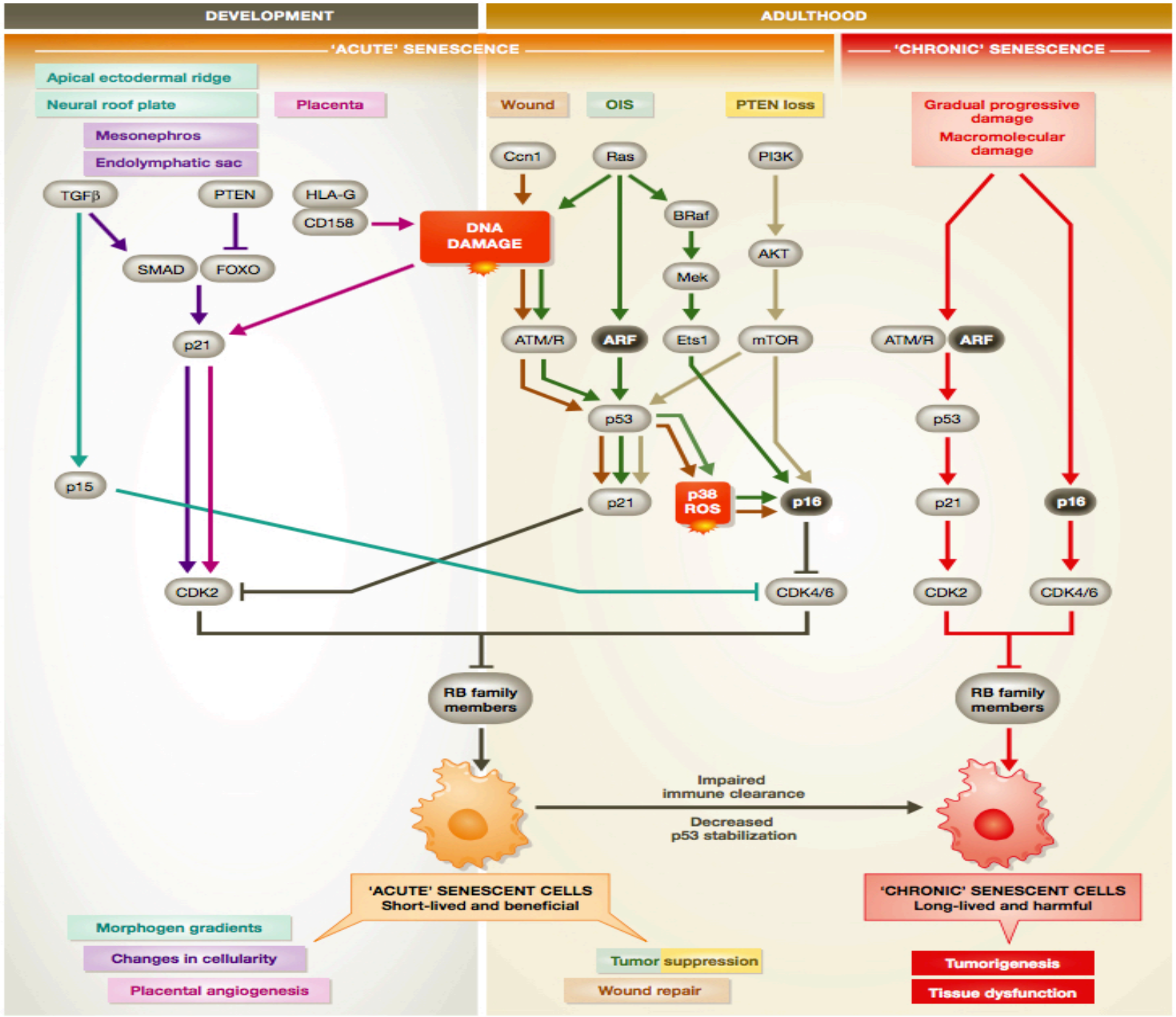
DEVELOPMENT
ADULTHOOD
'ACUTE' SENESCENCE
'CHRONIC' SENESCENCE
Apical ectodermal ridge
Neural roof plate
Placenta
Mesonephros
Endolymphatic sac
TGFβ
PTEN
HLA-G
CD158
SMAD
FOXO
p21
p15
CDK2
Wound
OIS
PTEN loss
Ccn1
Ras
PI3K
DNA DAMAGE
BRaf
AKT
Mek
ATM/R
ARF
Ets1
mTOR
p53
p21
p38 ROS
p16
CDK4/6
RB family members
Gradual progressive damage
Macromolecular damage
ATM/R
ARF
p53
p21
p16
CDK2
CDK4/6
RB family members
Impaired immune clearance
Decreased p53 stabilization
'ACUTE' SENESCENT CELLS
Short-lived and beneficial
'CHRONIC' SENESCENT CELLS
Long-lived and harmful
Morphogen gradients
Changes in cellularity
Placental angiogenesis
Tumor suppression
Wound repair
Tumorigenesis
Tissue dysfunction

Consequences of senescent cells on tissue

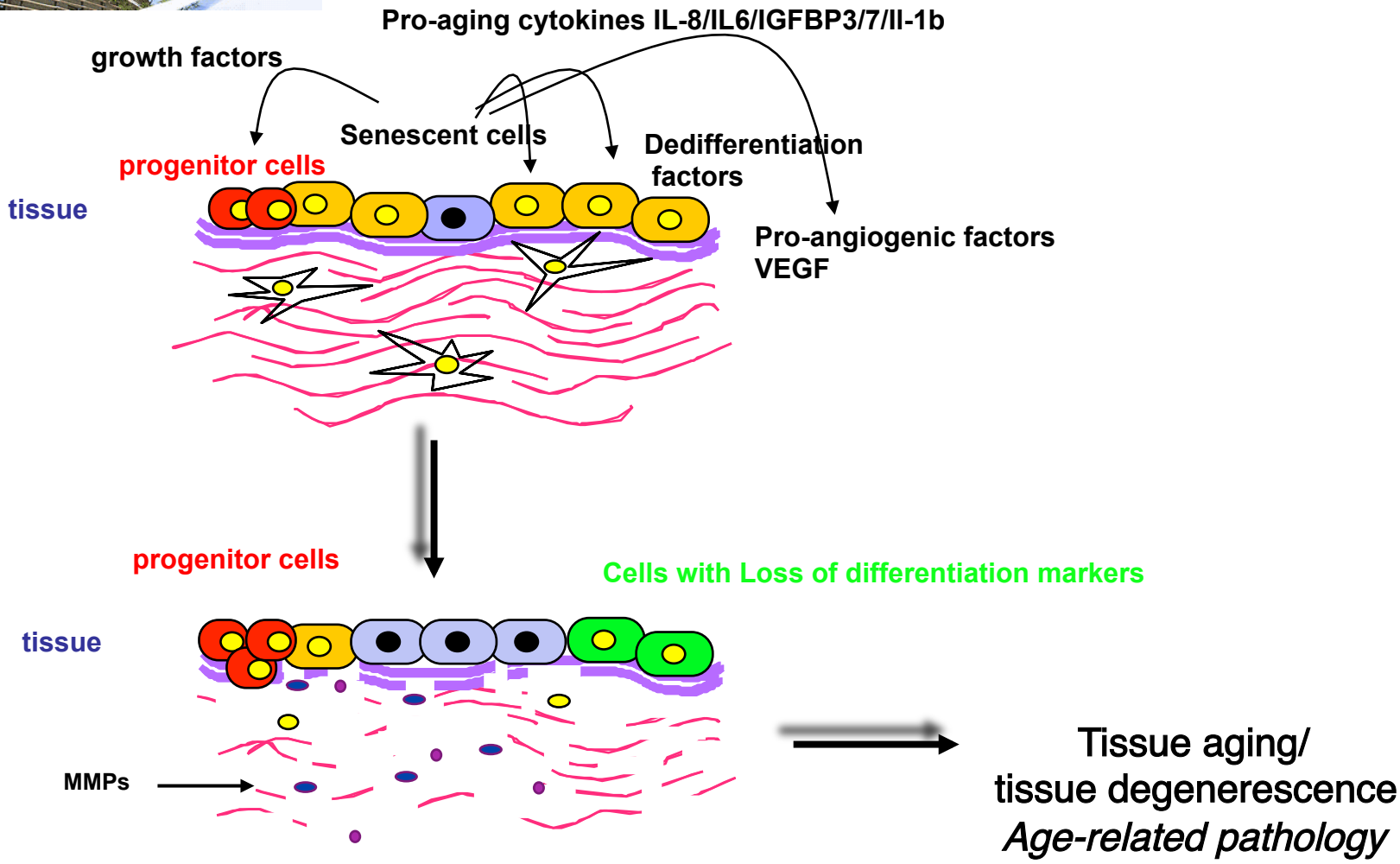

Senescent cells seem to contribute to age-related decline in tissue structure and function

Campisi, 2007

Mirs et senescence cellulaire

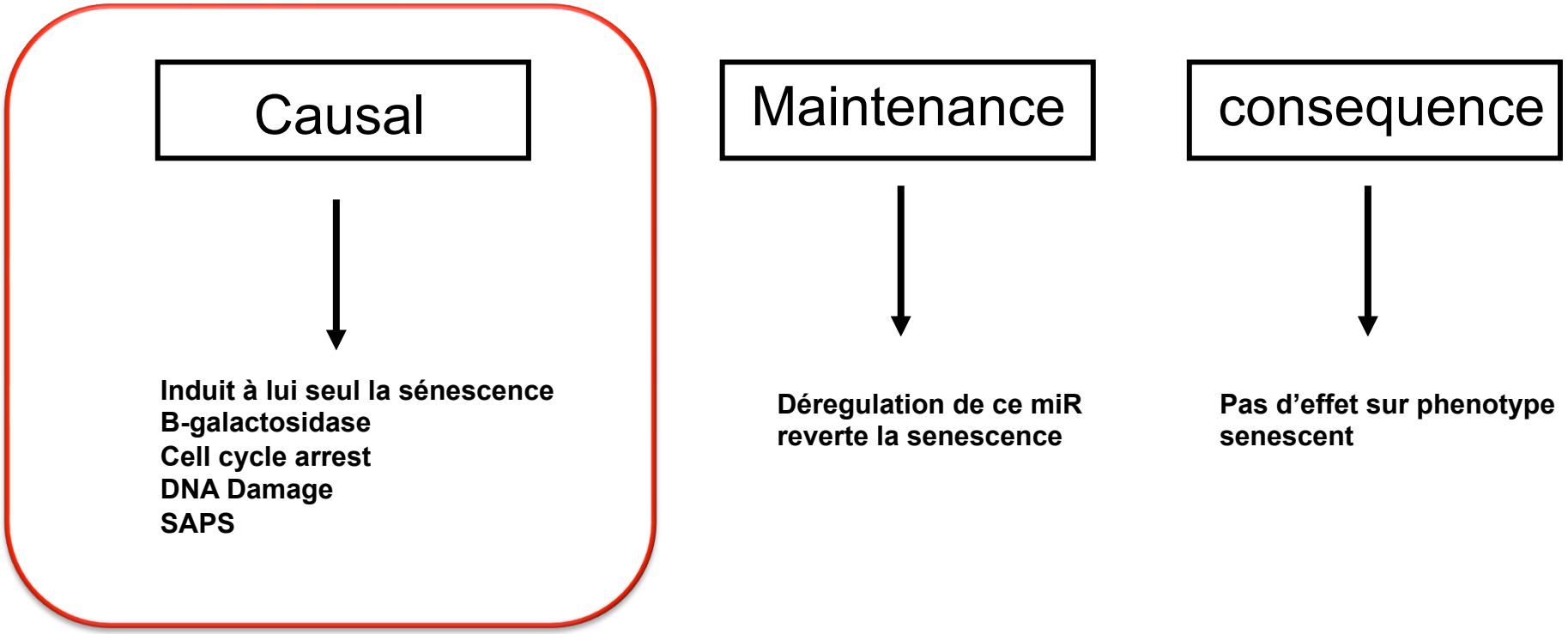

- **Loss of miRNA biogenesis induces p19Arf-p53 signaling and senescence in MEF**

- Rajini Mudhasani,1 Zhiqing Zhu,1 Gyorgy Hutvagner,2 Christine M. Eischen,4 Stephen Lyle,3 Lisa L. Hall,1 Jeanne B. Lawrence,1 Anthony N. Imbalzano,1 and Stephen N. Jones1,3

- J. Cell Biol. Vol. 181 No. 7 1055–1063

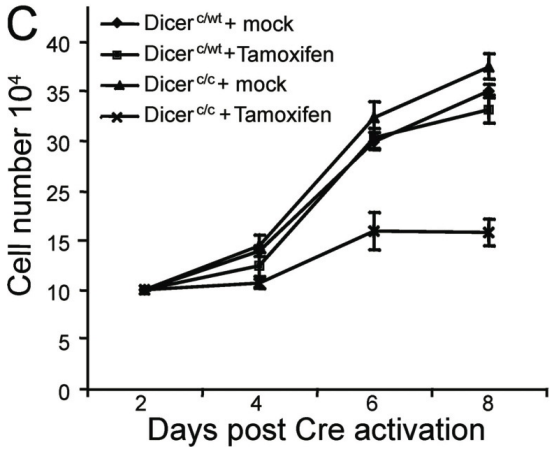

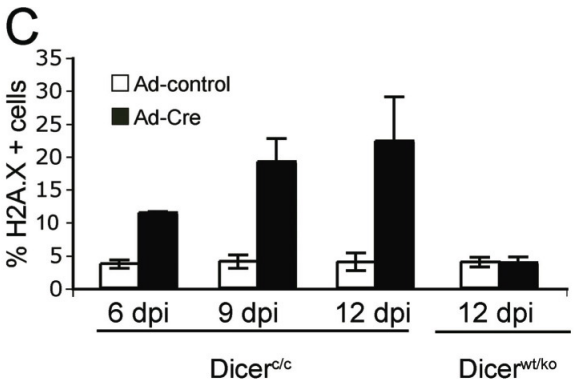

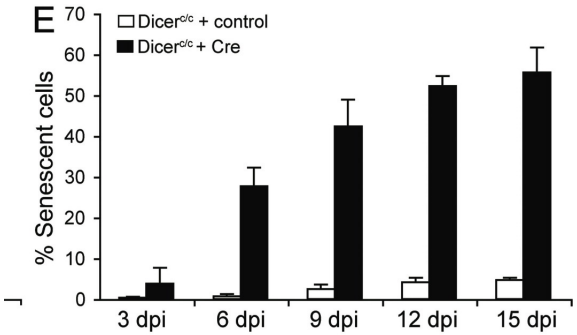

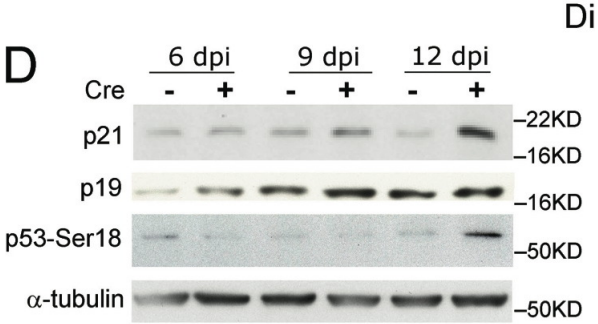

Cell Metabolism
Article

Role of MicroRNA Processing in Adipose Tissue in Stress Defense and Longevity

Marcelo A. Mori,[1] Prashant Raghavan,[2] Thomas Thomou,[1,3] Jeremie Boucher,[1] Stacey Robida-Stubbs,[2] Yazmin Macotela,[1] Steven J. Russell,[1] James L. Kirkland,[3] T. Keith Blackwell,[2] and C. Ronald Kahn[1,*]
[1]Section on Integrative Physiology and Metabolism
[2]Section on Islet Cell and Regenerative Biology
Joslin Diabetes Center, Harvard Medical School, Boston, MA 02215, USA
[3]Robert and Arlene Kogod Center on Aging, Mayo Clinic, Rochester, MN 55905, USA
*Correspondence: c.ronald.kahn@joslin.harvard.edu
http://dx.doi.org/10.1016/j.cmet.2012.07.017

Inactivation de dicer induit la senescence d'adipocytes in vitro

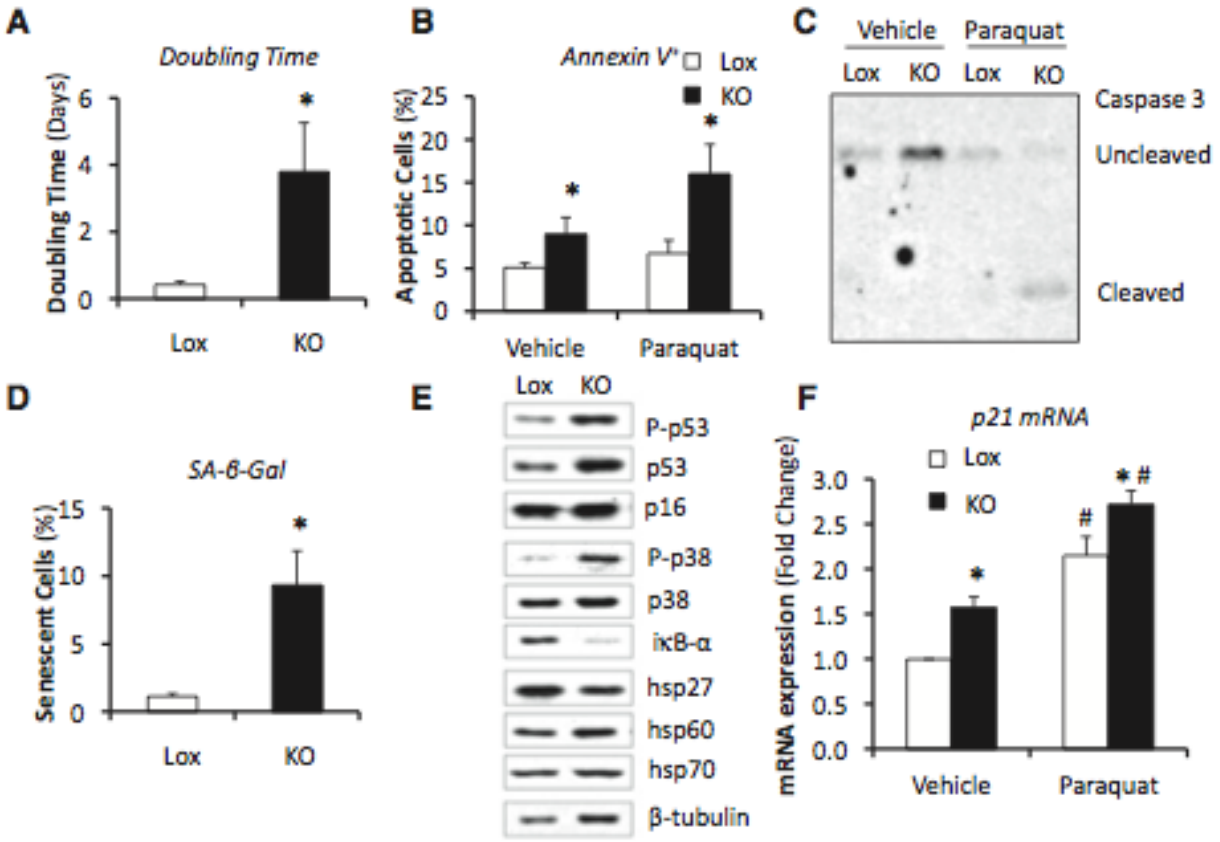

Régulation de MKK4 par plusieurs Mirs

Increased MKK4 abundance with replicative senescence is linked to the joint reduction of multiple microRNAs

Bernard S. Marasa,[1] Subramanya Srikantan,[1] Kiyoshi Masuda,[1] Kotb Abdelmohsen,[1] Yuki Kuwano,[1] Xiaoling Yang,[1]

Jennifer L. Martindale,[1] Carrie W. Rinker-Schaeffer,[2] and Myriam Gorospee

Sci Signal. 2009 October 27; 2(94): ra69.

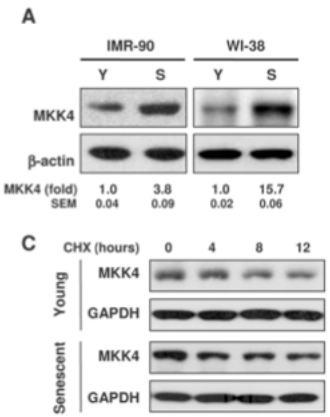

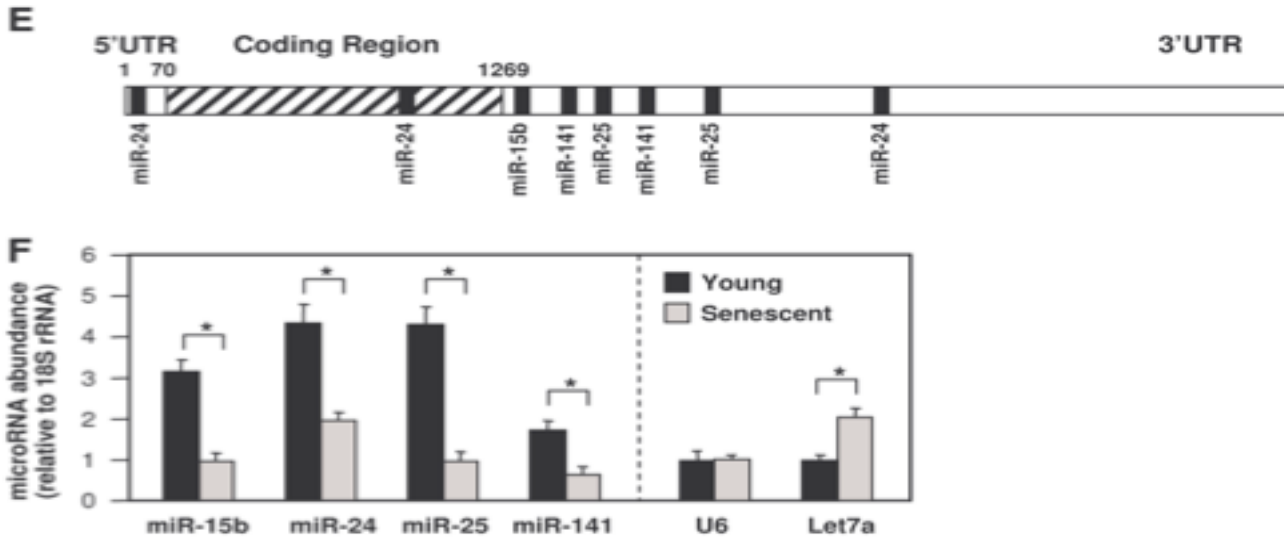

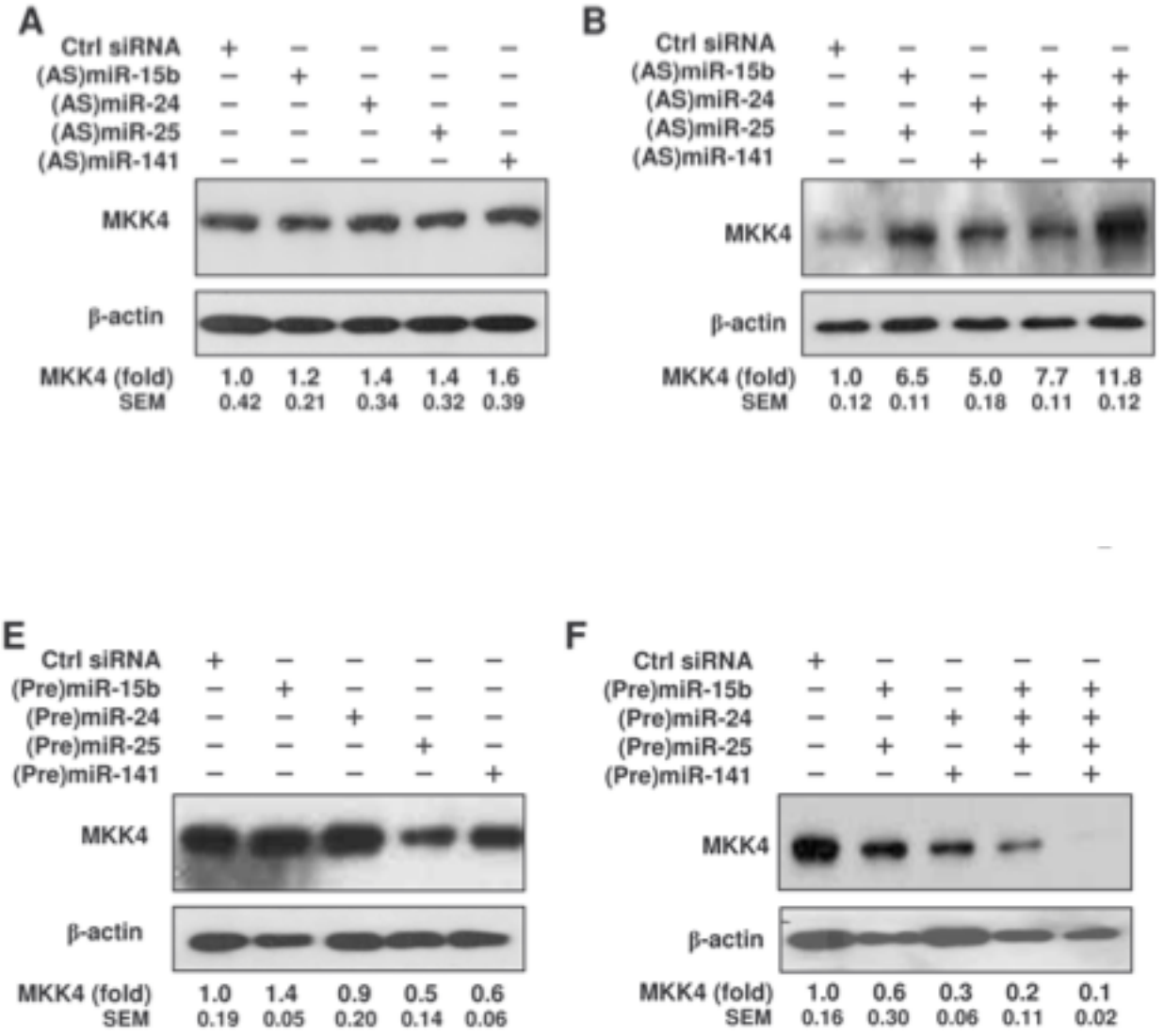
A
Ctrl siRNA + – – – –
(AS)miR-15b – + – – –
(AS)miR-24 – – + – –
(AS)miR-25 – – – + –
(AS)miR-141 – – – – +
MKK4
β-actin
MKK4 (fold) 1.0 1.2 1.4 1.4 1.6
SEM 0.42 0.21 0.34 0.32 0.39
B
Ctrl siRNA + – – – –
(AS)miR-15b – + – + +
(AS)miR-24 – – + + +
(AS)miR-25 – + – + +
(AS)miR-141 – – + – +
MKK4
β-actin
MKK4 (fold) 1.0 6.5 5.0 7.7 11.8
SEM 0.12 0.11 0.18 0.11 0.12
E
Ctrl siRNA + – – – –
(Pre)miR-15b – + – – –
(Pre)miR-24 – – + – –
(Pre)miR-25 – – – + –
(Pre)miR-141 – – – – +
MKK4
β-actin
MKK4 (fold) 1.0 1.4 0.9 0.5 0.6
SEM 0.19 0.05 0.20 0.14 0.06
F
Ctrl siRNA + – – – –
(Pre)miR-15b – + – + +
(Pre)miR-24 – – + + +
(Pre)miR-25 – + – + +
(Pre)miR-141 – – + – +
MKK4
β-actin
MKK4 (fold) 1.0 0.6 0.3 0.2 0.1
SEM 0.16 0.30 0.06 0.11 0.02

Mirs et senescence cellulaire

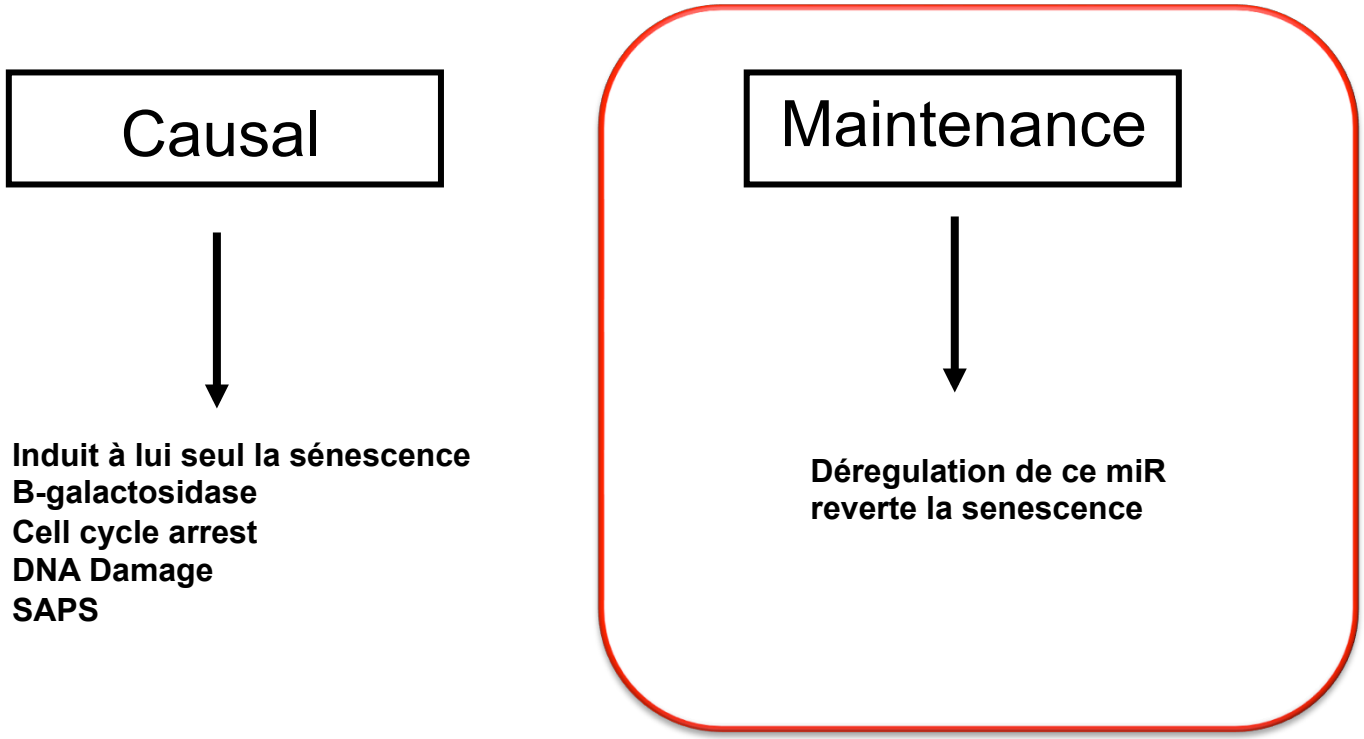

Cell

A Genetic Screen Implicates miRNA-372 and miRNA-373 As Oncogenes in Testicular Germ Cell Tumors

P. Mathijs Voorhoeve,[1,5] Carlos le Sage,[1,5] Mariette Schrier,[1] Ad J.M. Gillis,[2] Hans Stoop,[2] Remco Nagel,[1] Ying-Poi Liu,[1] Josyanne van Duijse,[1] Jarno Drost,[1] Alexander Griekspoor,[1] Eitan Zlotorynski,[1] Norikazu Yabuta,[4] Gabriella De Vita,[3] Hiroshi Nojima,[4] Leendert H.J. Looijenga,[2] and Reuven Agami[1,*]

[1] Division of Tumour Biology, The Netherlands Cancer Institute, Amsterdam, The Netherlands

[2] Department of Pathology, Erasmus University Medical Center Rotterdam, Daniel den Hoed Cancer Center, Josephine Nefkens Institute, Rotterdam, The Netherlands

[3] Dipartimento di Biologia e Patologia Cellulare e Molecolare, Università Federico II, CEINGE Biotecnologie Avanzate, Naples, Italy

[4] Department of Molecular Genetics, Osaka University, Japan

[5] These authors contributed equally to this work.

*Contact: r.agami@nki.nl

DOI 10.1016/j.cell.2006.02.037

A

Oncogenic RAS → Primary cells → senescence

Oncogenic RAS → Primary cells lacking p53 → growth

Oncogenic RAS → Primary cells +miRNA? → growth

C

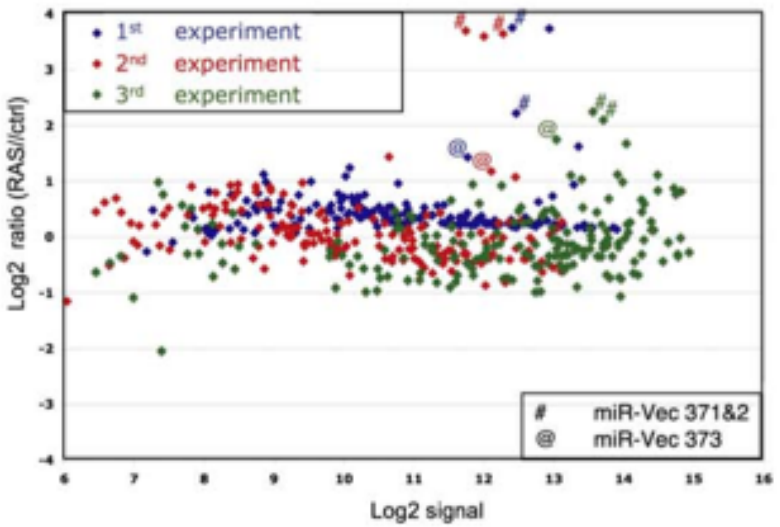

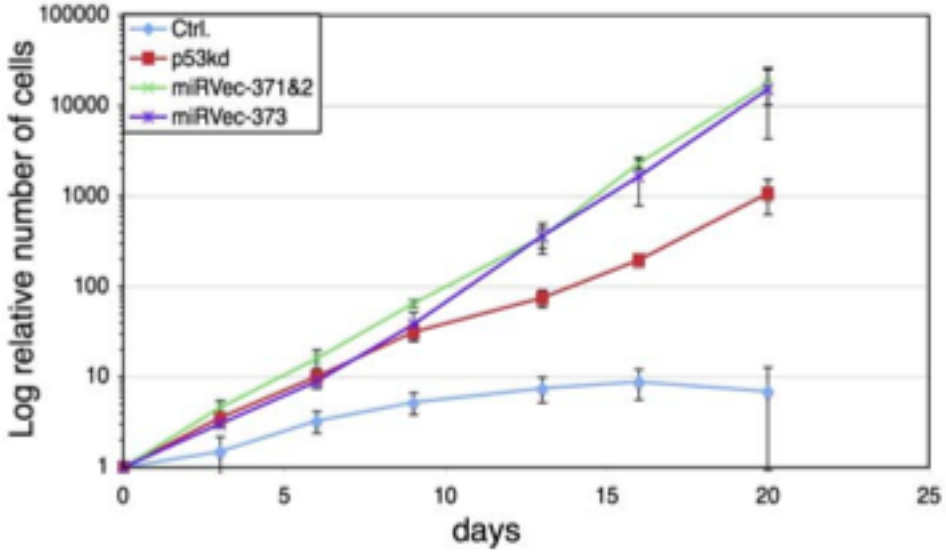
Ctrl.
p53kd
miRVec-371&2
miRVec-373
Log relative number of cells
100000
10000
1000
100
10
1
0
5
10
15
20
25
days

H

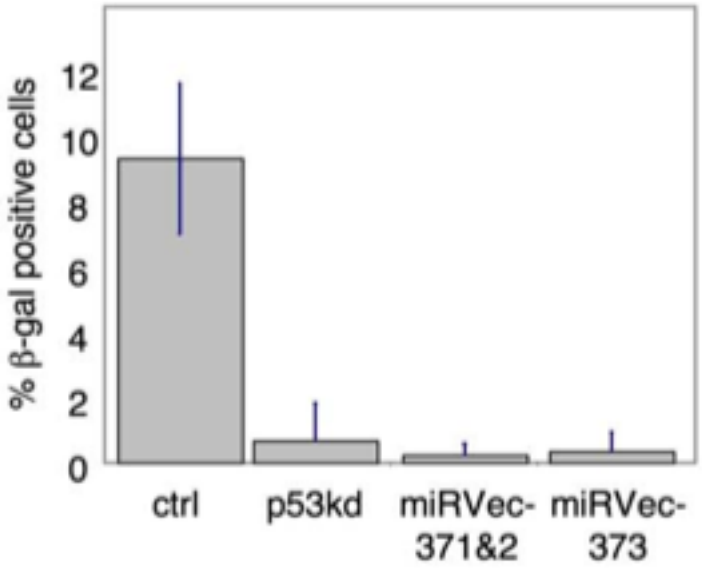
% β-gal positive cells
12
10
8
6
4
2
0
ctrl
p53kd
miRVec-371&2
miRVec-373

En résumé

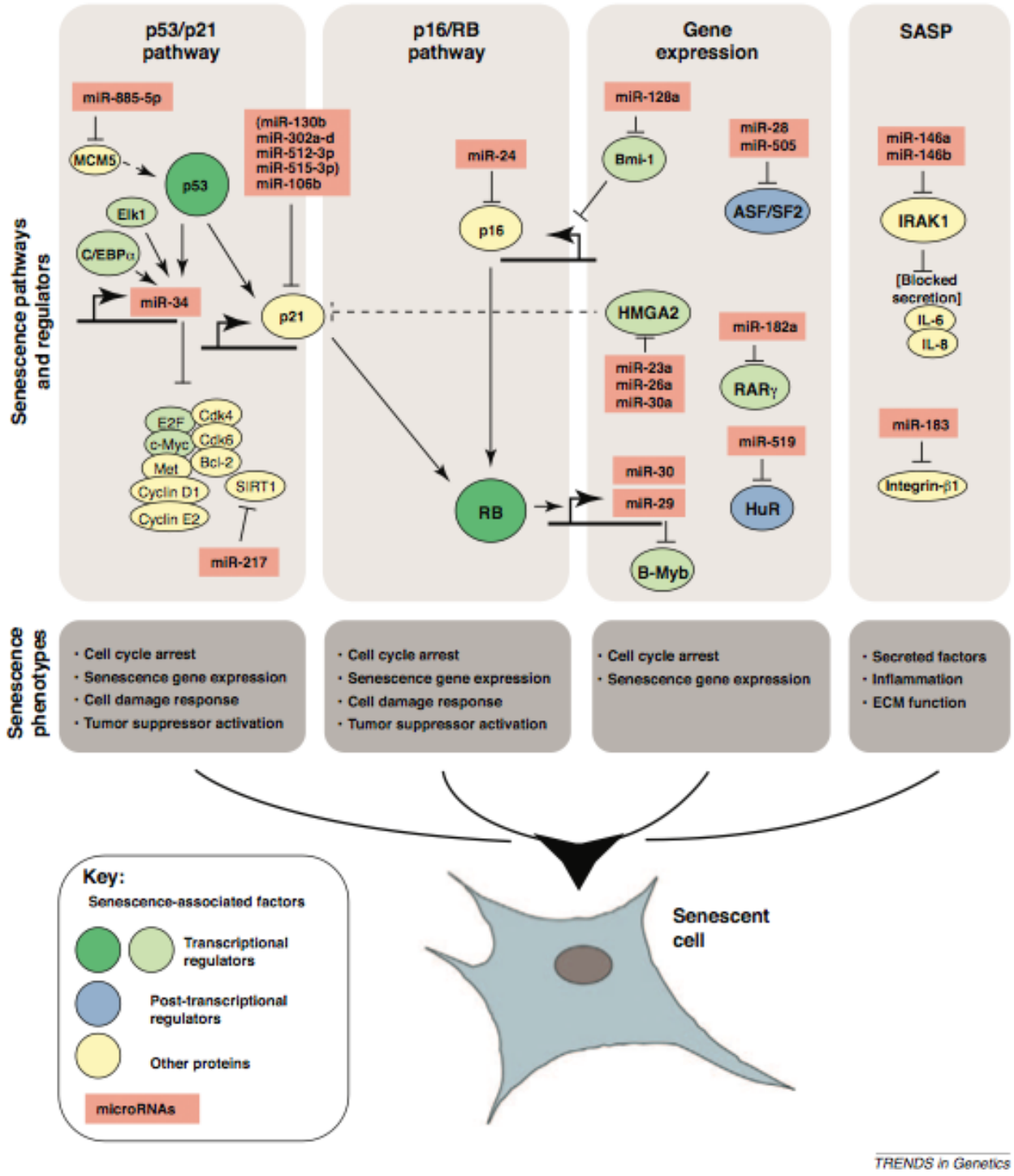
p53/p21 pathway
p16/RB pathway
Gene expression
SASP
Senescence pathways and regulators
miR-885-5p
MCM5
p53
(miR-130b
miR-302a-d
miR-512-3p
miR-515-3p)
miR-106b
Elk1
C/EBPα
miR-34
p21
E2F
Cdk4
c-Myc
Cdk6
Met
Bcl-2
Cyclin D1
SIRT1
Cyclin E2
miR-217
miR-24
p16
RB
miR-128a
Bmi-1
HMGA2
miR-23a
miR-26a
miR-30a
miR-30
miR-29
B-Myb
miR-28
miR-505
ASF/SF2
miR-182a
RARγ
miR-519
HuR
miR-146a
miR-146b
IRAK1
[Blocked secretion]
IL-6
IL-8
miR-183
Integrin-β1
Senescence phenotypes
· Cell cycle arrest
· Senescence gene expression
· Cell damage response
· Tumor suppressor activation
· Cell cycle arrest
· Senescence gene expression
· Cell damage response
· Tumor suppressor activation
· Cell cycle arrest
· Senescence gene expression
· Secreted factors
· Inflammation
· ECM function
Key:
Senescence-associated factors
Transcriptional regulators
Post-transcriptional regulators
Other proteins
microRNAs
Senescent cell
TRENDS in Genetics

Environmental Factors
(mechanical stress
Cytokines, UVs)

intrinsec Factors
(oxidative stress-
DNA repair defects)

DNA Damage

Cellular Senescence

Epigenetic changes

Changes in gene expression

Specific Secretome (SMS)

Tissue Aging
(loss of function)

Stem-cell Aging

Systemic Aging

Organismal aging

Adapted from Brunet A. et al, Nature 2007

Exemple: pathologies osteo-articulaire associées à l'âge

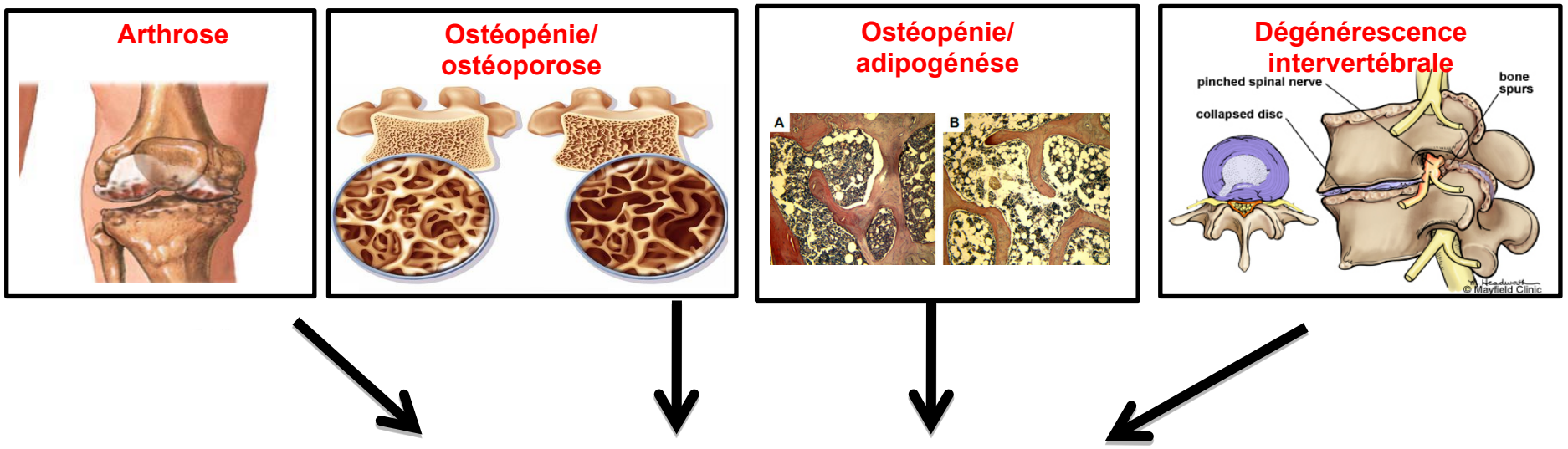

Pathologies ostéo-articulaires du sujet âgé associant la sénescence cellulaire et la perte de l'homéostasie des tissus

Osteoarthritis: an age-related disease

Healthy

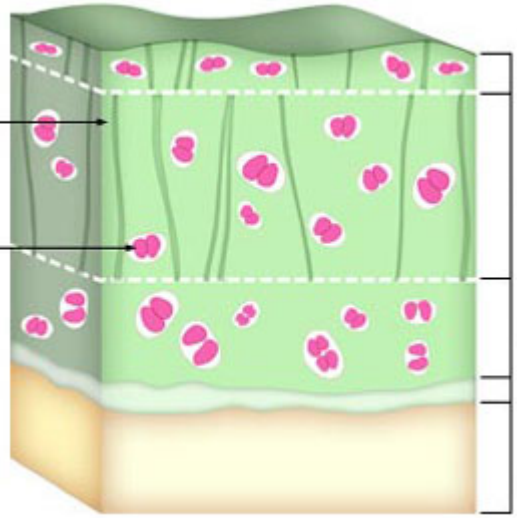

OA

Telomere Shortening (Martin et al., 2001)
$p16^{INK4a}$ accumulation(Zhou et al., 2004)
p53 activation (Dai et al., 2006)
ROS production (Yudoh et al., 2005)
Secretome Associated Senescence Phenotype (Calamia et al., 2011)

Senescence-like phenotype

- Localization: Knees, hands and hips

- Not only age, but others factors are involved in OA predisposition: such as genetics factors or obesity …

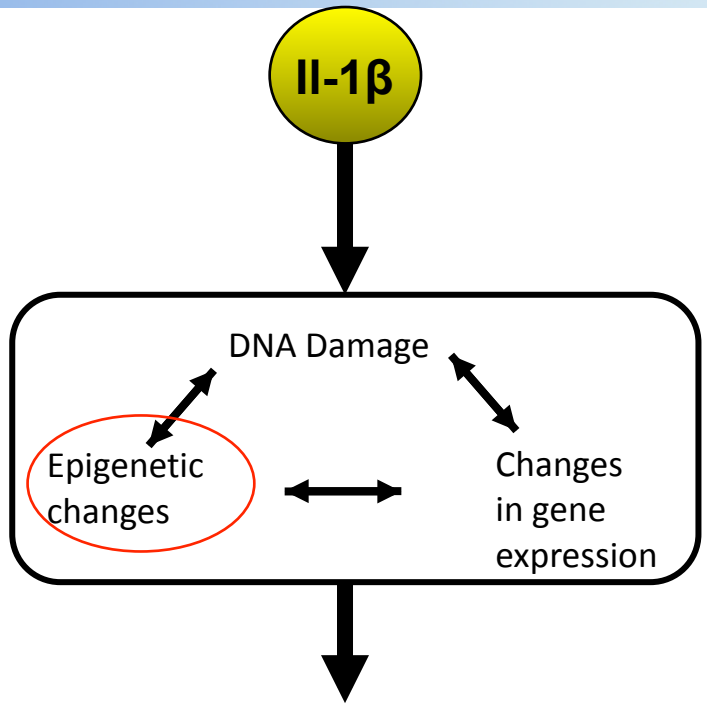

Senescence-like phenotype of chondrocytes

Cartilage premature aging with expression of p16ink4a (loss of function)

Osteoarthritis

How to identify miR deregulated in OA ?

We treated human primary chondrocytes with Il-1b cytokine in order to reproduce the major senescent phenotypes associated with OA

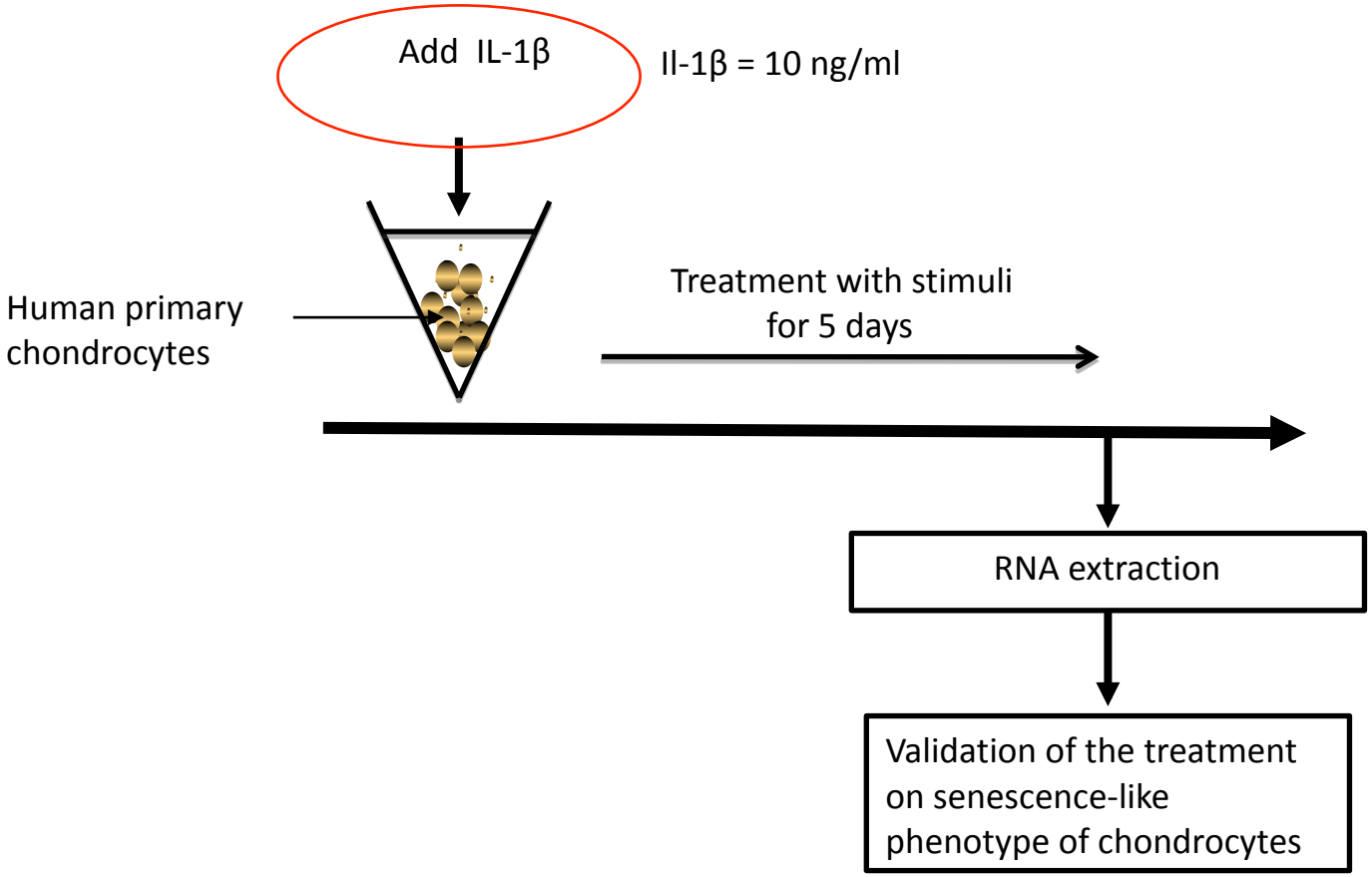

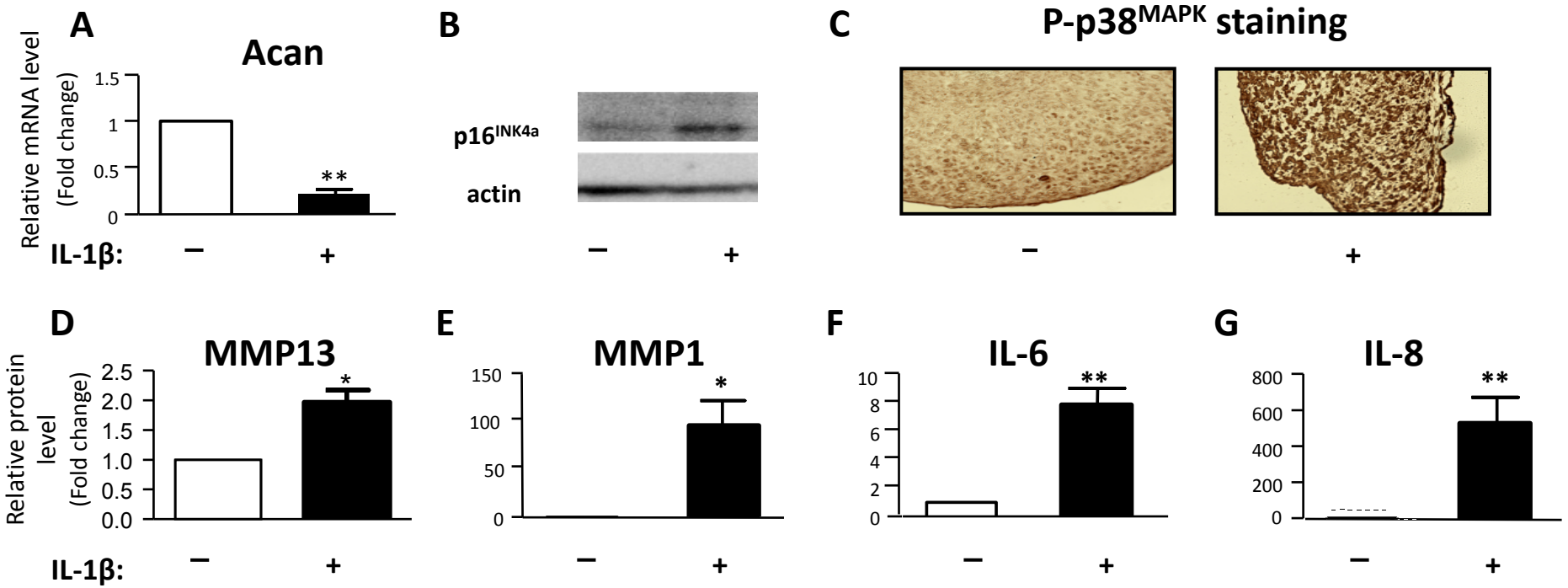

Senescence-like phenotypes of chondrocytes treated by IL-1b

p16INK4a overexpression is sufficient to induce MMP1 and MMP13

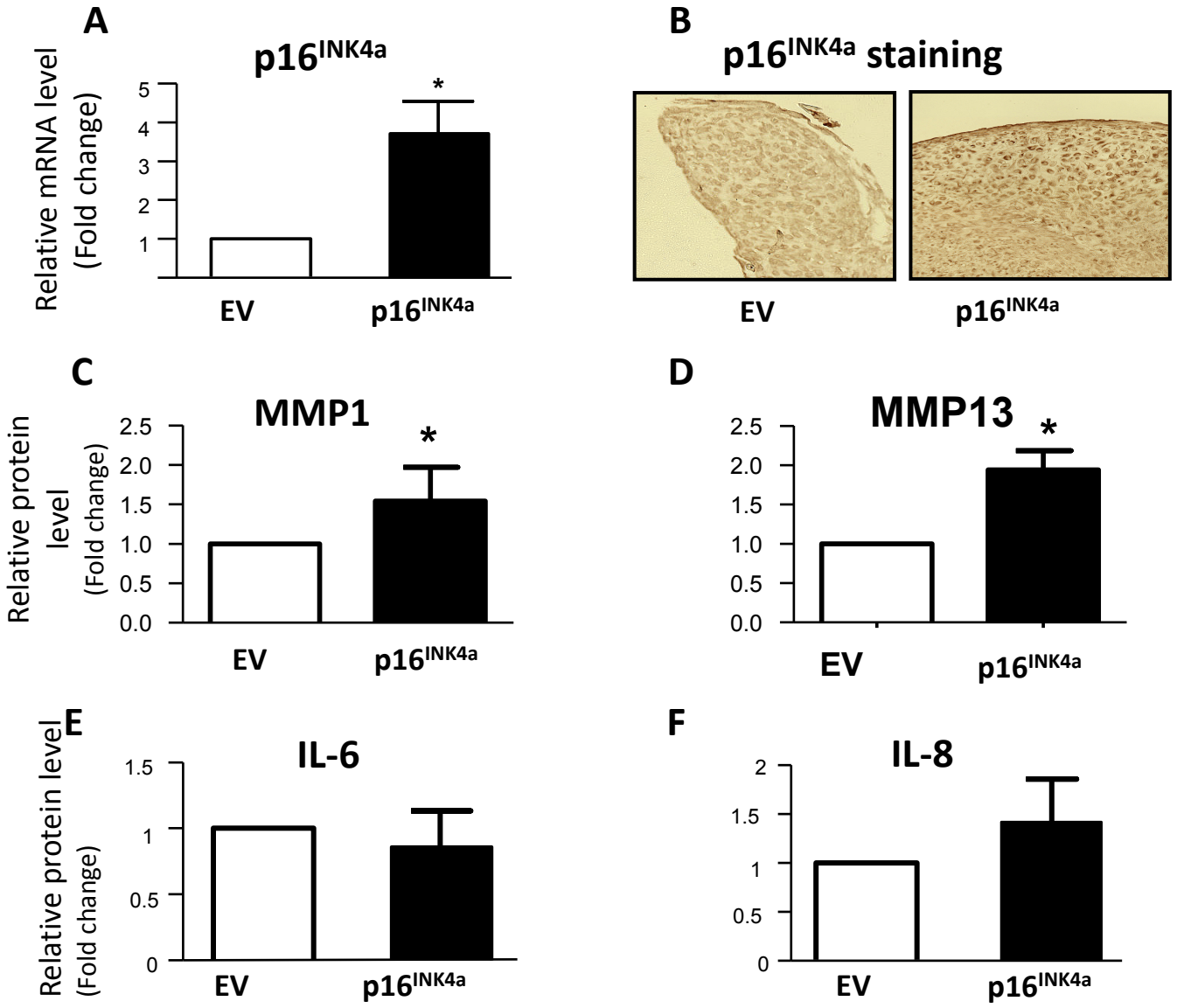

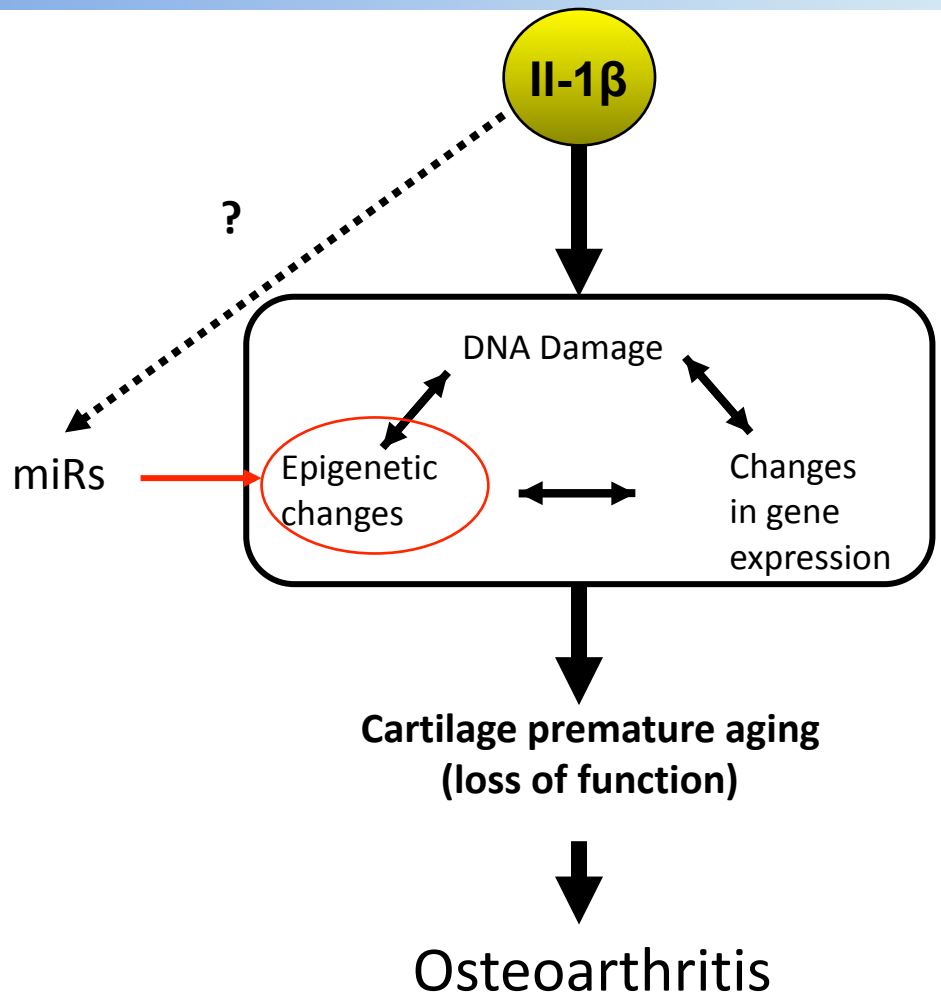

Senescence-like phenotype of chondrocytes

Analyse des puces

A

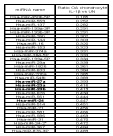

miR-24-1/2 clusters are down regulated

$p16^{INK4A}$ protein:

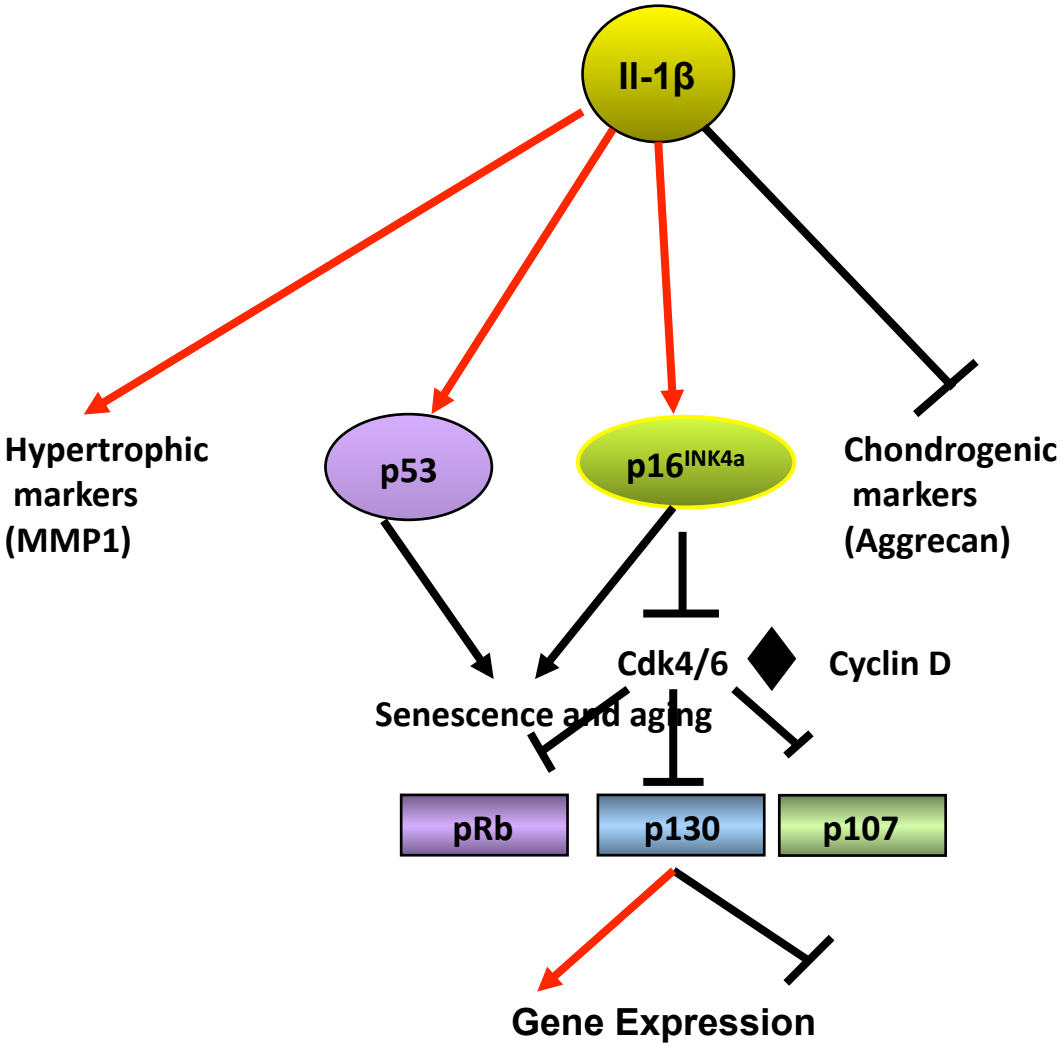

$p16^{INK4a}$ mRNA

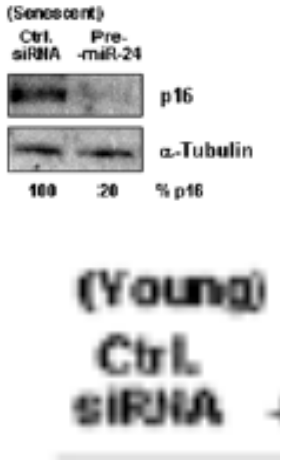

(Lal et al., PLOS one,2008)

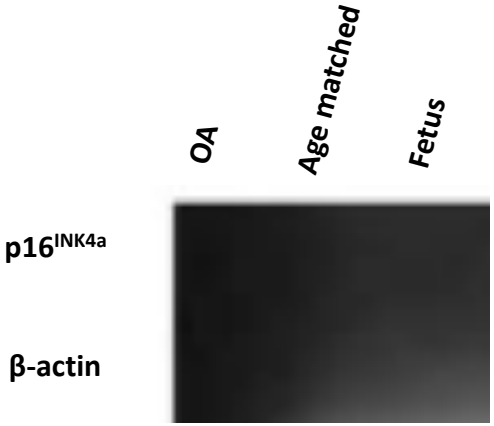

(Zhou et al., Rheumatology, 2004)

A

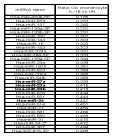

B

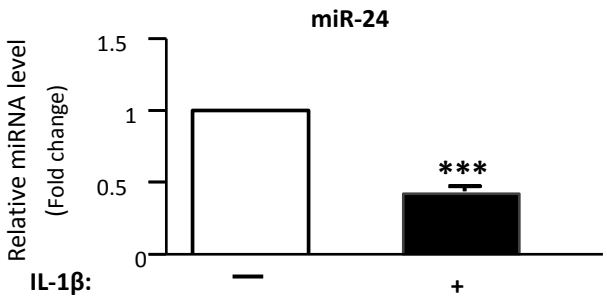

C

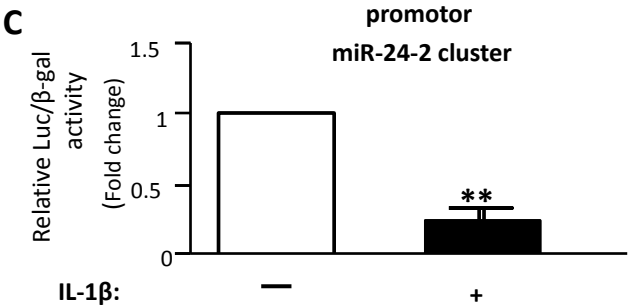

D

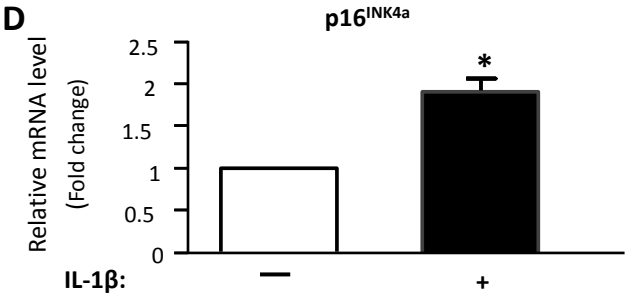

Reverse correlation between miR-24 and p16INK4a expression

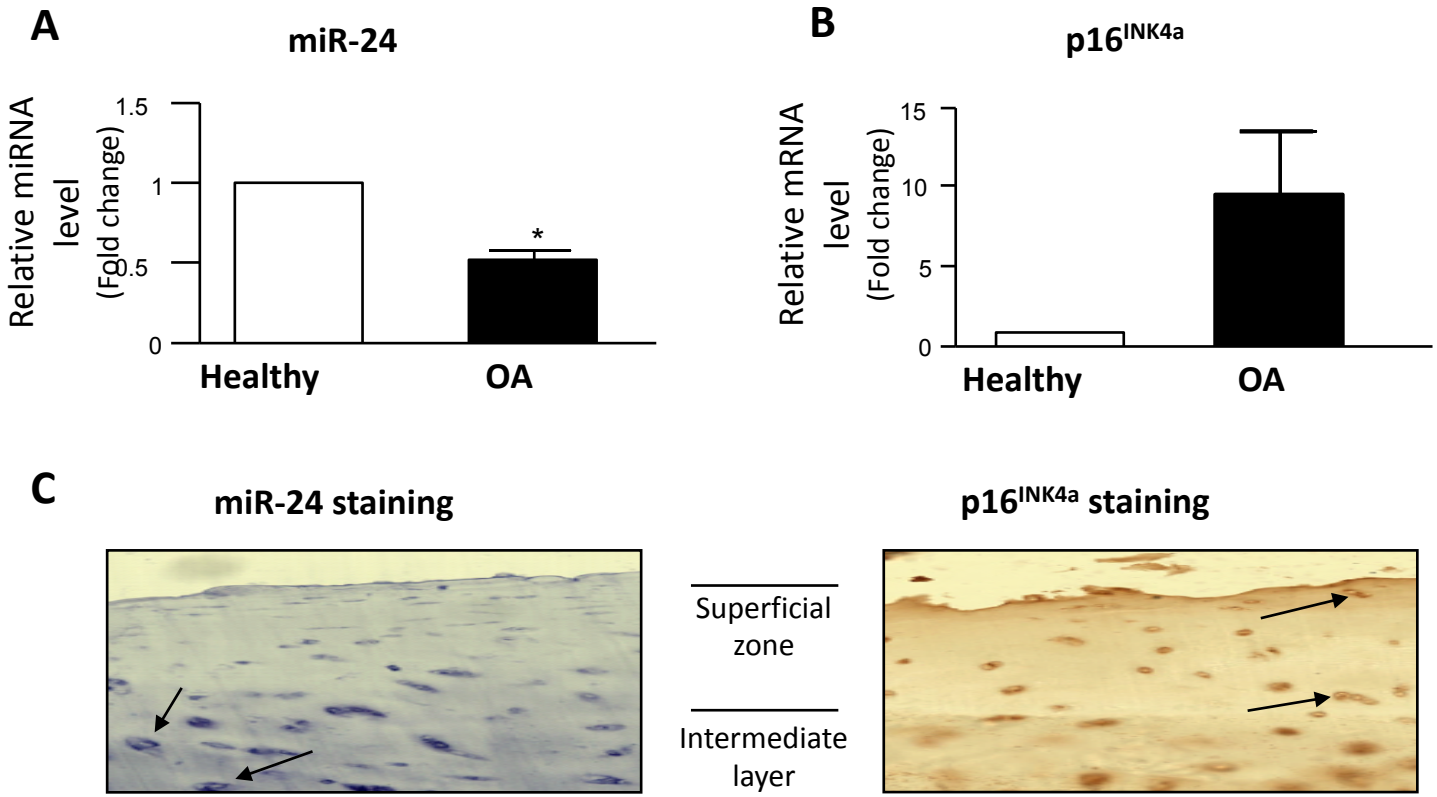

Reverse correlation between miR-24 and p16INK4a expression in human cartilage

U844

What is the impact of miR-24 down regulation on senescence-like phenotype found in OA?

Transfection with antagomir control or against miR-24

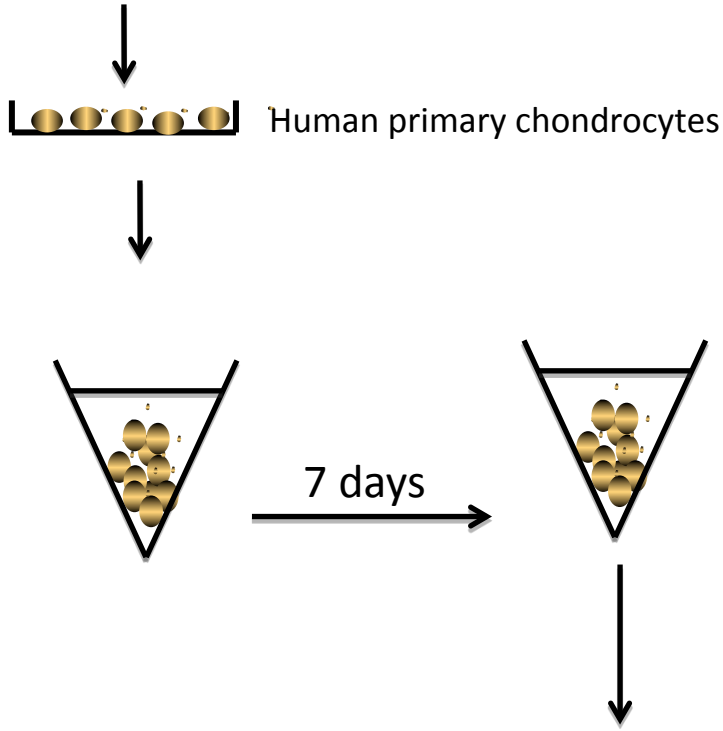

RT-qPCR and Elisa for expression of miR-24, $p16^{INK4a}$ chondrogenic markers and MMP1

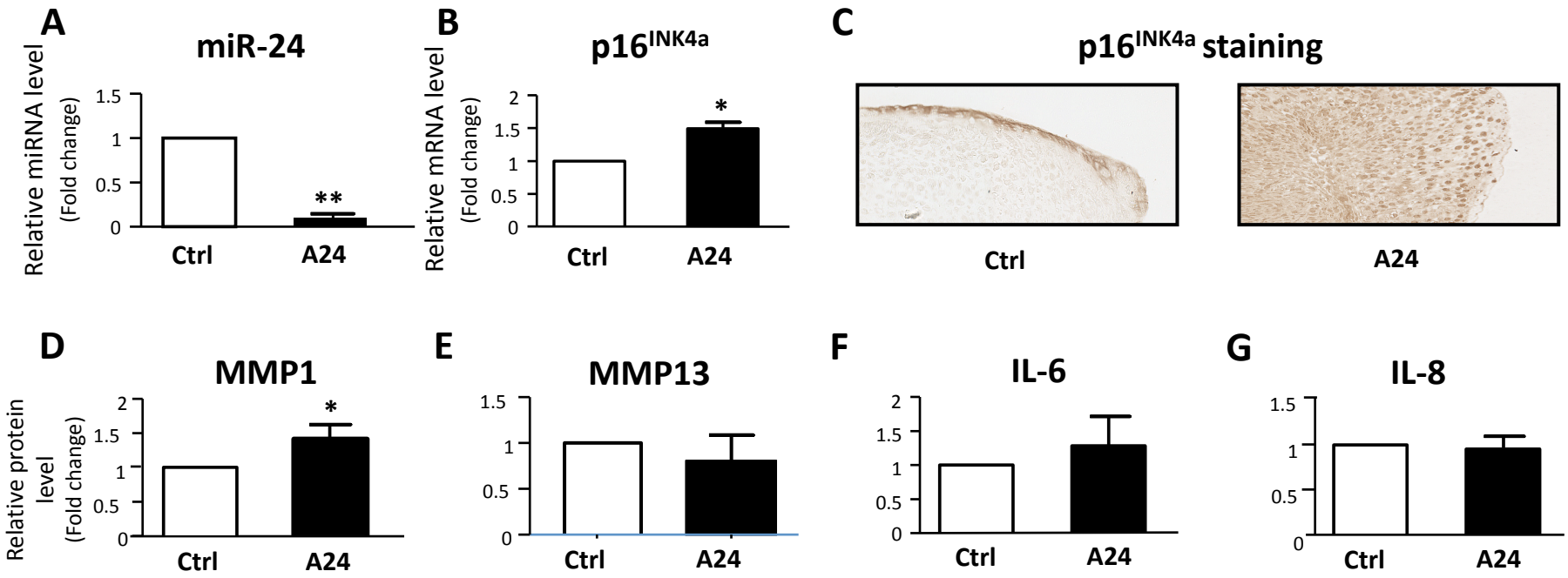

Down regulation of miR-24 is sufficient to induce p16INK4A and MMP1

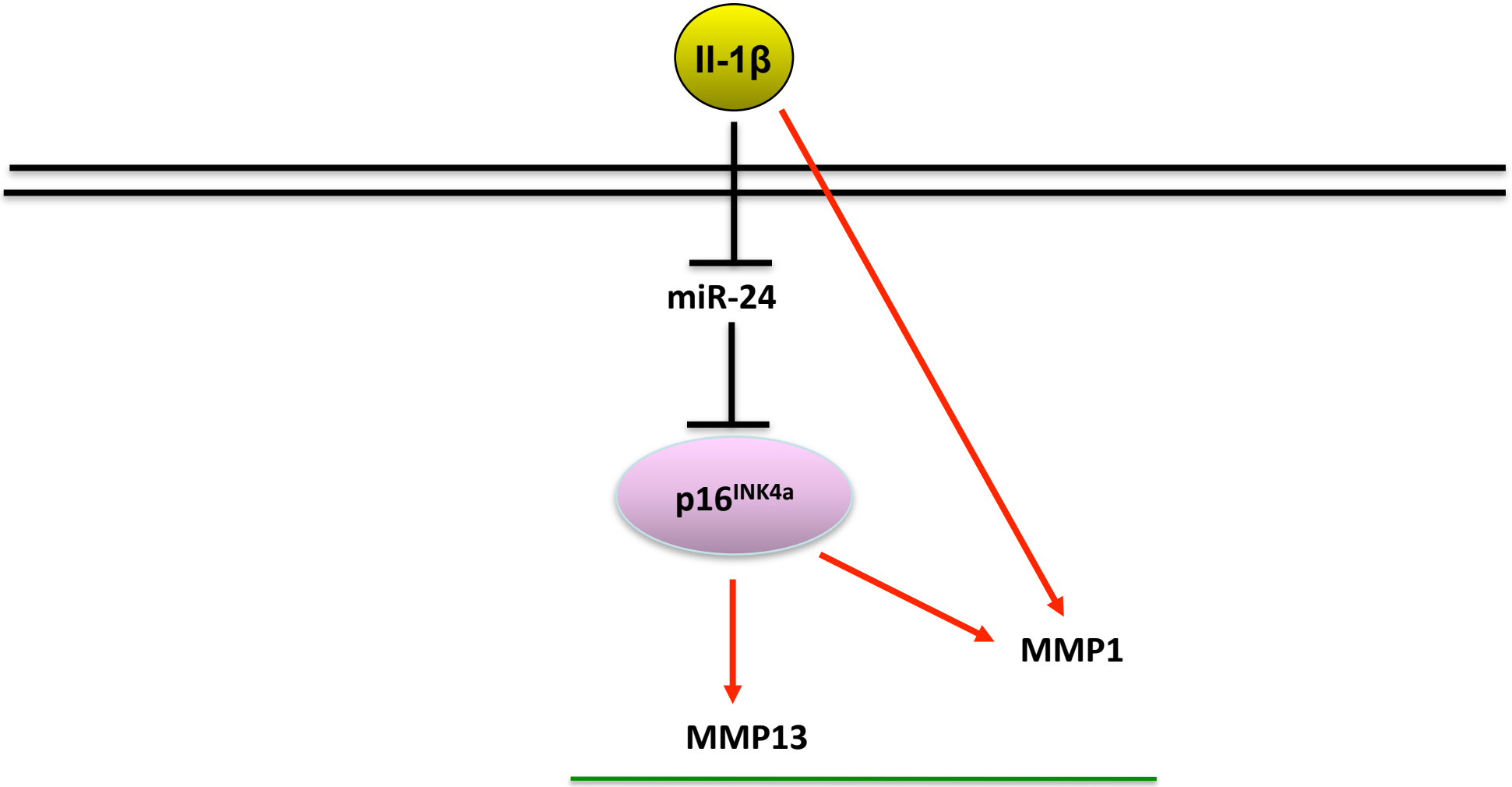
Il-1β
miR-24
p16INK4a
MMP1
MMP13
Hypertrophic phenotype associated
with cartilage degenerescence in OA

Environmental Factors
(mechanical stress
Cytokines, UVs)

intrinsec Factors
(oxidative stress-
DNA repair defects)

DNA Damage

Epigenetic changes

Changes in gene expression

Cellular Senescence

Specific Secretome (SMS)

Tissue Aging
(loss of function)

Stem-cell Aging

Systemic Aging

Organismal aging

Adapted from Brunet A. et al, Nature 2007

Exemple: pathologies osteo-articulaire associées à l'âge

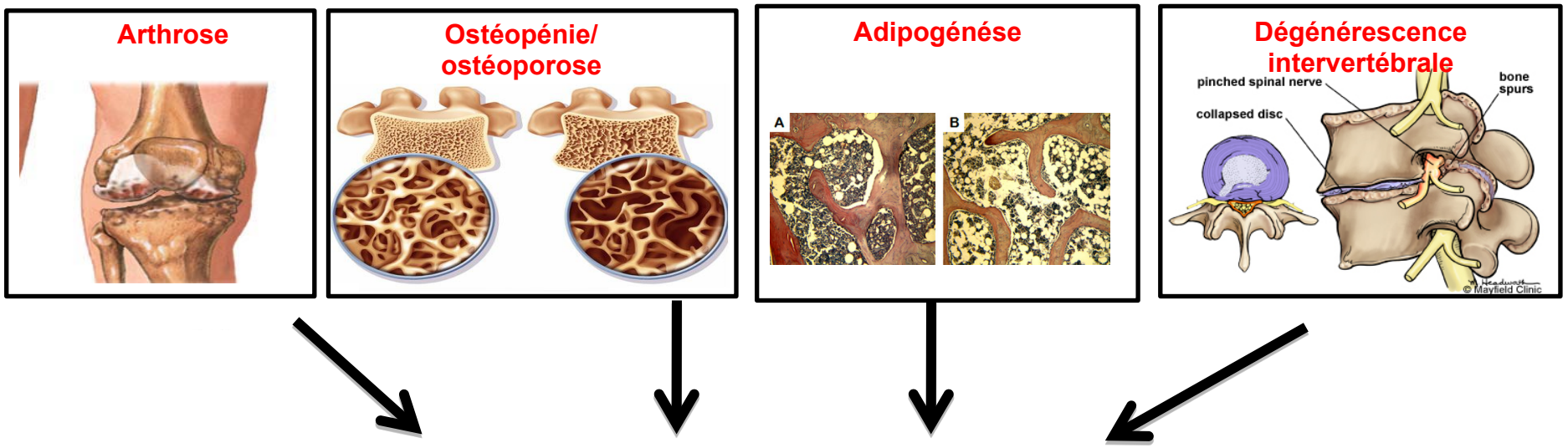

Pathologies ostéo-articulaires du sujet âgé associant la sénescence cellulaire et la perte de l'homéostasie des tissus

Les CSM (cellules souches mesenchymataueses: cellules souches ostéo-articulaires

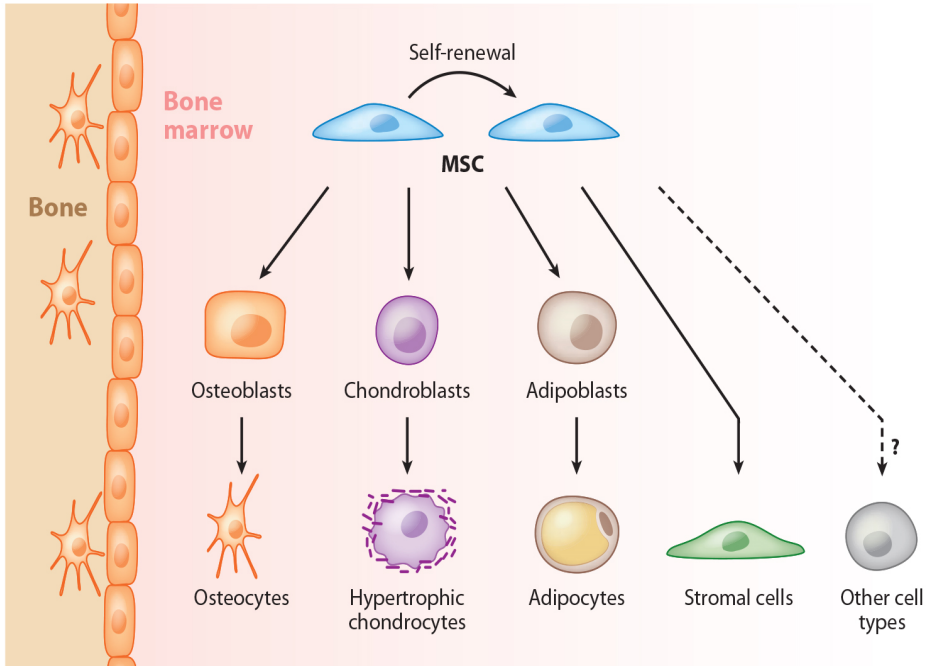

Caractéristiques

• localisation: M osseuse, placenta, tissu adipeux

•Adhérence au plastique

• marqueurs de surface

positive: CD90 CD105 et CD73 (nestin+)
negative: CD11b CD14 CD34 CD45

Fonctions intrinséques

•Capacité d'autorenouvellement (CfU-F)

•capacité de différenciation osteo/adipo/chondro

Fonctions extrinséques

•Support stromal à d'autres cellules souches (niche HSC) ou à des tissus différenciés

•Immuno-modulation

The Journal of Clinical Investigation RESEARCH ARTICLE

MicroRNA-188 regulates age-related switch between osteoblast and adipocyte differentiation

Chang-Jun Li,[1,2] Peng Cheng,[1,3] Meng-Ke Liang,[1] Yu-Si Chen,[1] Qiong Lu,[1] Jin-Yu Wang,[1] Zhu-Ying Xia,[1] Hou-De Zhou,[1] Xu Cao,[2] Hui Xie,[1] Er-Yuan Liao,[1] and Xiang-Hang Luo[1]

[1]Institute of Endocrinology and Metabolism, The Second Xiangya Hospital of Central South University, Changsha, Hunan, China. [2]Department of Orthopaedic Surgery, Johns Hopkins University School of Medicine, Baltimore, Maryland, USA. [3]Department of Gerontology, The First Hospital Affiliated to Nanjing Medical University, Nanjing, Jiangsu, China.

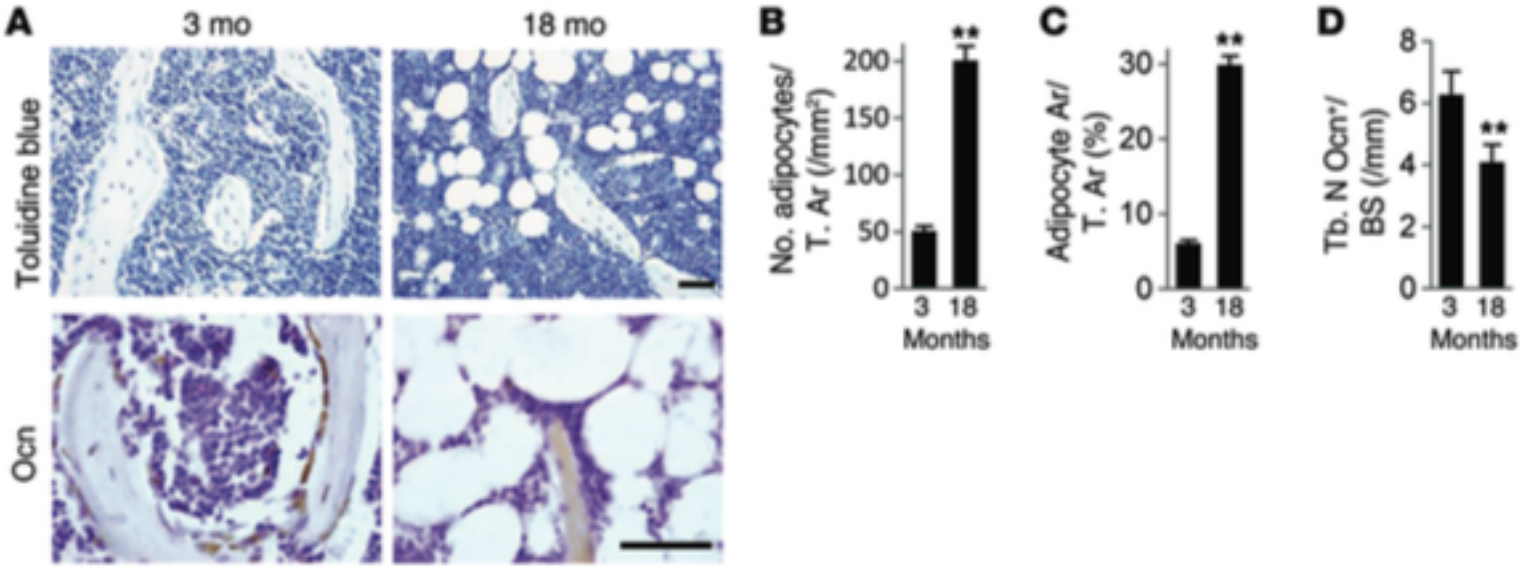

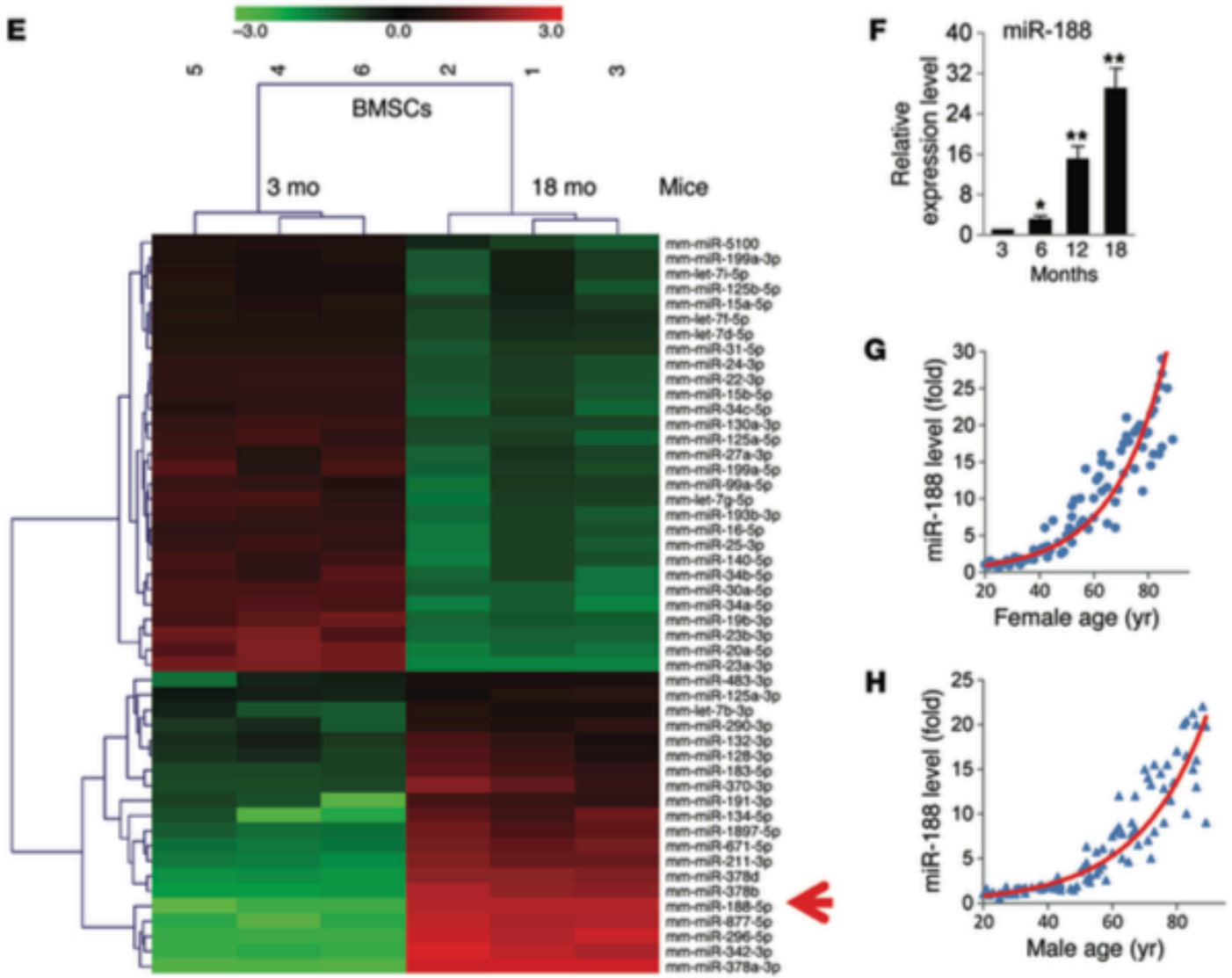

Figure 1. Aging induces miR-188 expression in BMSCs. (**A**–**D**) Representative images of toluidine blue (T.) staining (**A**, top) and osteocalcin (Ocn) immunohistochemical staining (**A**, bottom) and quantification of number and area (Ar) of adipocytes (**B** and **C**) and number of osteoblasts (**D**) in distal femora from 3-month-old and 18-month-old female C57BL/6 mice. Tb. N, trabecular number. Scale bars: 100 μm. $n = 6$ per group. (**E**) Microarray profiling results of deregulated miRNAs in BMSCs from young and aged mice. (**F**) qRT-PCR analysis of the levels of miR-188 expression in BMSCs derived from the mice at different ages. $n = 6$ per group. (**G** and **H**) Age-associated changes of miR-188 levels in BMSCs from 85 human females (**G**) and 85 males (**H**). Data shown as mean ± SD. $^*P < 0.05$, $^{**}P < 0.01$ (**B**–**D**, Student's *t* test; **F**, ANOVA).

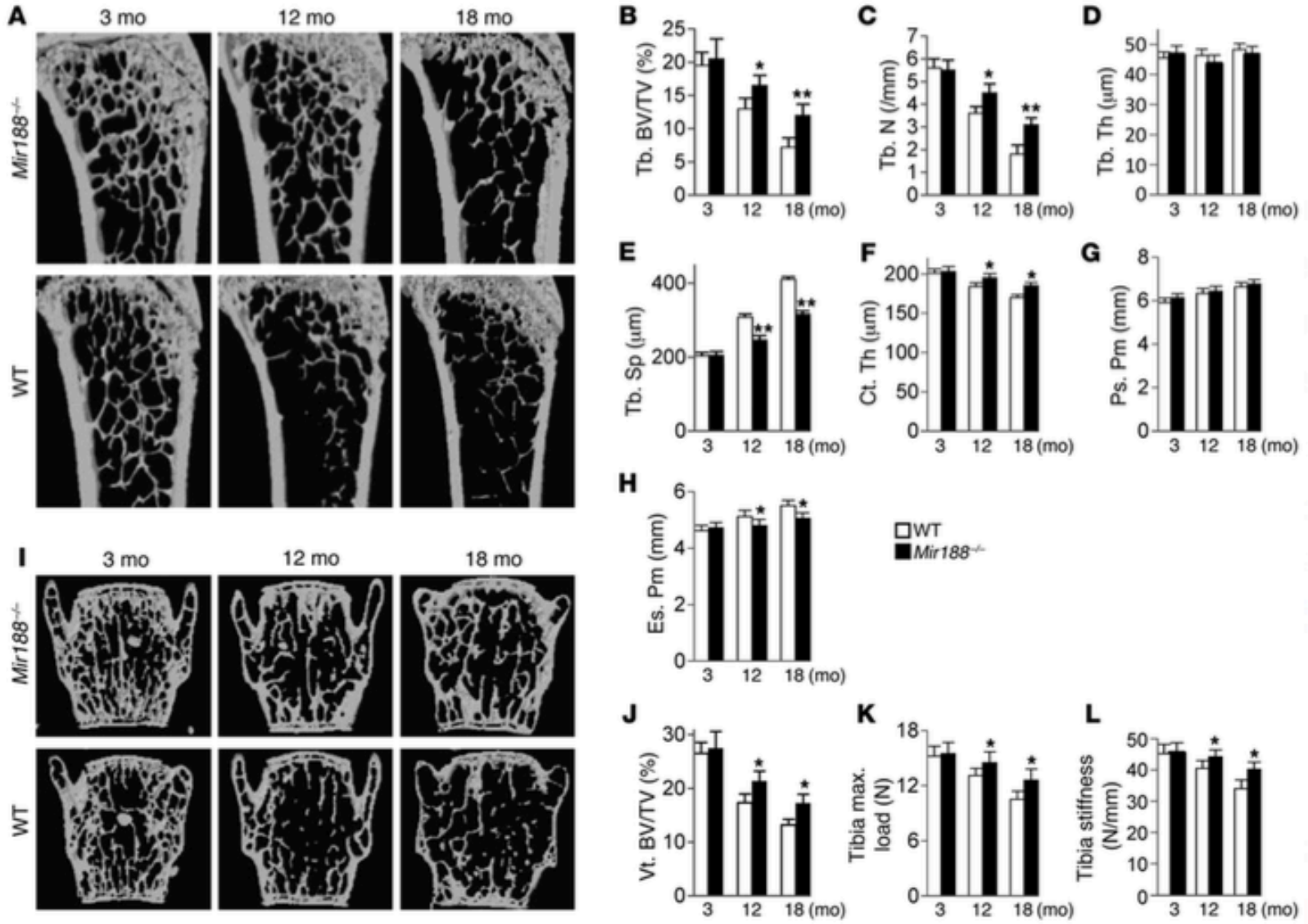

Figure 2. *Mir188*$^{-/-}$ mice exhibit reduced age-associated bone loss. (**A**–**H**) Representative microcomputed tomography (μCT) images (**A**) and quantitative μCT analysis of trabecular (**B**–**E**) and cortical (**F**–**H**) bone microarchitecture in femora from 3-, 12-, and 18-month-old WT and miR-188 knockout (*Mir188*$^{-/-}$) mice. $n = 6$ per group. Tb. BV/TV, trabecular bone volume per tissue volume; Tb. Th, trabecular thickness; Tb. Sp, trabecular separation; Ct. Th, cortical thickness; Ps. Pm, periosteal perimeter; Es. Pm, endosteal perimeter. (**I** and **J**) Representative μCT images (**I**) and quantification of the ratio of bone volume to tissue volume (**J**) of L4 vertebrae (Vt. BV/TV). $n = 6$ per group. (**K** and **L**) Three-point bending measurement of tibia maximum load (**K**) and stiffness (**L**). $n = 5$ per group. Data shown as mean ± SD. $^{*}P < 0.05$, $^{**}P < 0.01$ (Student's *t* test).

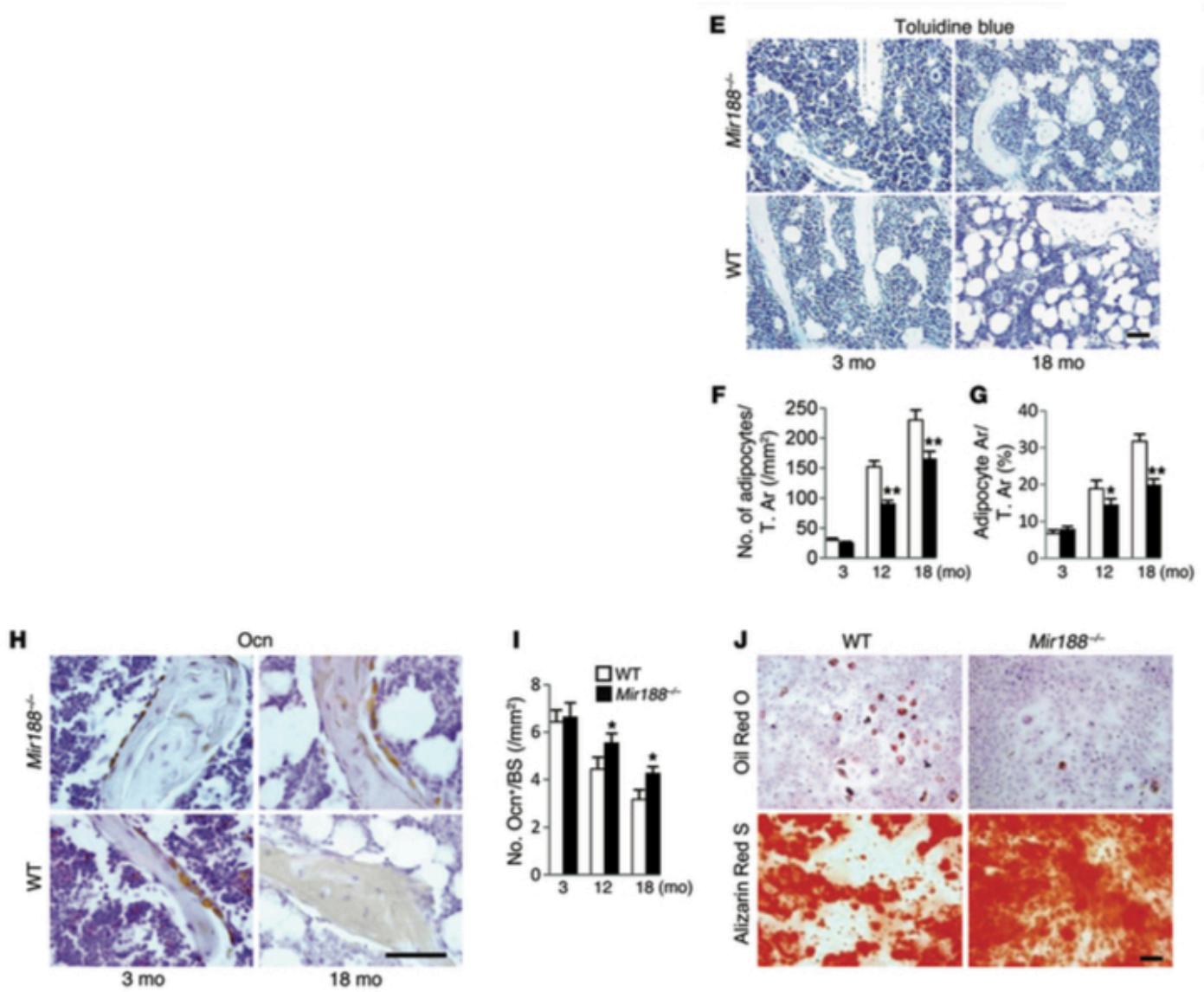

Figure 3. *Mir188*$^{-/-}$ mice show higher osteoblastic bone formation and lower marrow fat accumulation in aged mice. (**A**) Representative images of calcein double labeling of trabecular (Tb), endosteal (Eb), and periosteal bone (Pb) with quantification (**B**–**D**) of bone formation rate per bone surface (BFR/BS) in femora of 18-month-old WT and *Mir188*$^{-/-}$ mice. Scale bar: 50 μm. $n = 6$ per group. (**E**) Representative images of toluidine blue staining with quantification of number and area of adipocytes in distal femora (**F** and **G**). Scale bar: 100 μm. (**H**) Representative images of osteocalcin immunohistochemical staining with quantification of number of osteoblasts in distal femora (**I**). Scale bar: 100 μm. $n = 6$ per group. (**J**) Representative images of Oil Red O staining of lipids (top) and Alizarin Red S staining of matrix mineralization (bottom) in BMSCs from *Mir188*$^{-/-}$ mice and WT mice cultured in adipogenesis induction medium for 14 days and osteogenesis induction medium for 21 days, respectively. Scale bar: 100 μm. Data are representative of 3 independent experiments. Data shown as mean ± SD. $^{*}P < 0.05$, $^{**}P < 0.01$ (Student's *t* test).

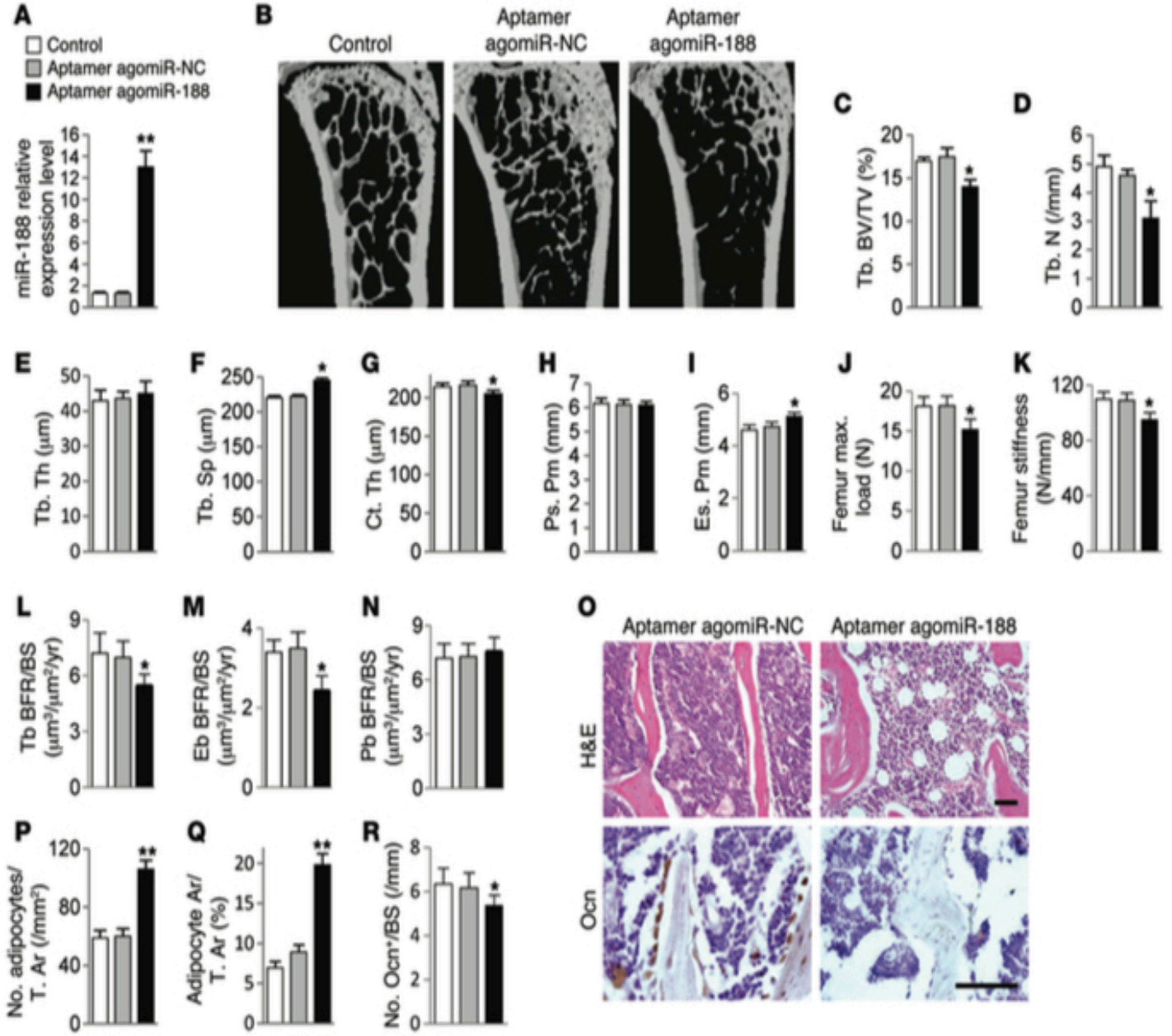

Figure 5. Mice with BMSC-specific overexpression of miR-188 using aptamer delivery system exhibit reduced bone formation and increased marrow fat accumulation. (**A**) qRT-PCR analysis of levels of miR-188 expression in BMSCs of mice with aptamer delivery. NC, negative control. $n = 6$ per group. (**B–I**) Representative μCT images (**B**) and quantitative μCT analysis of trabecular (**C–F**) and cortical bone (**G–I**) microarchitecture in femora from aptamer-treated mice. $n = 10$. (**J** and **K**) Three-point bending measurement of femur maximum load (**J**) and stiffness (**K**). $n = 5$ per group. (**L–N**) Calcein double labeling–based quantification of bone formation rate per bone surface (BFR/BS) in femora. $n = 5$ per group. (**O–R**) Representative images of H&E staining (**O**, top) and osteocalcin immunohistochemical staining (**O**, bottom) and quantification of number and area of adipocytes (**P** and **Q**) and number of osteoblasts (**R**)

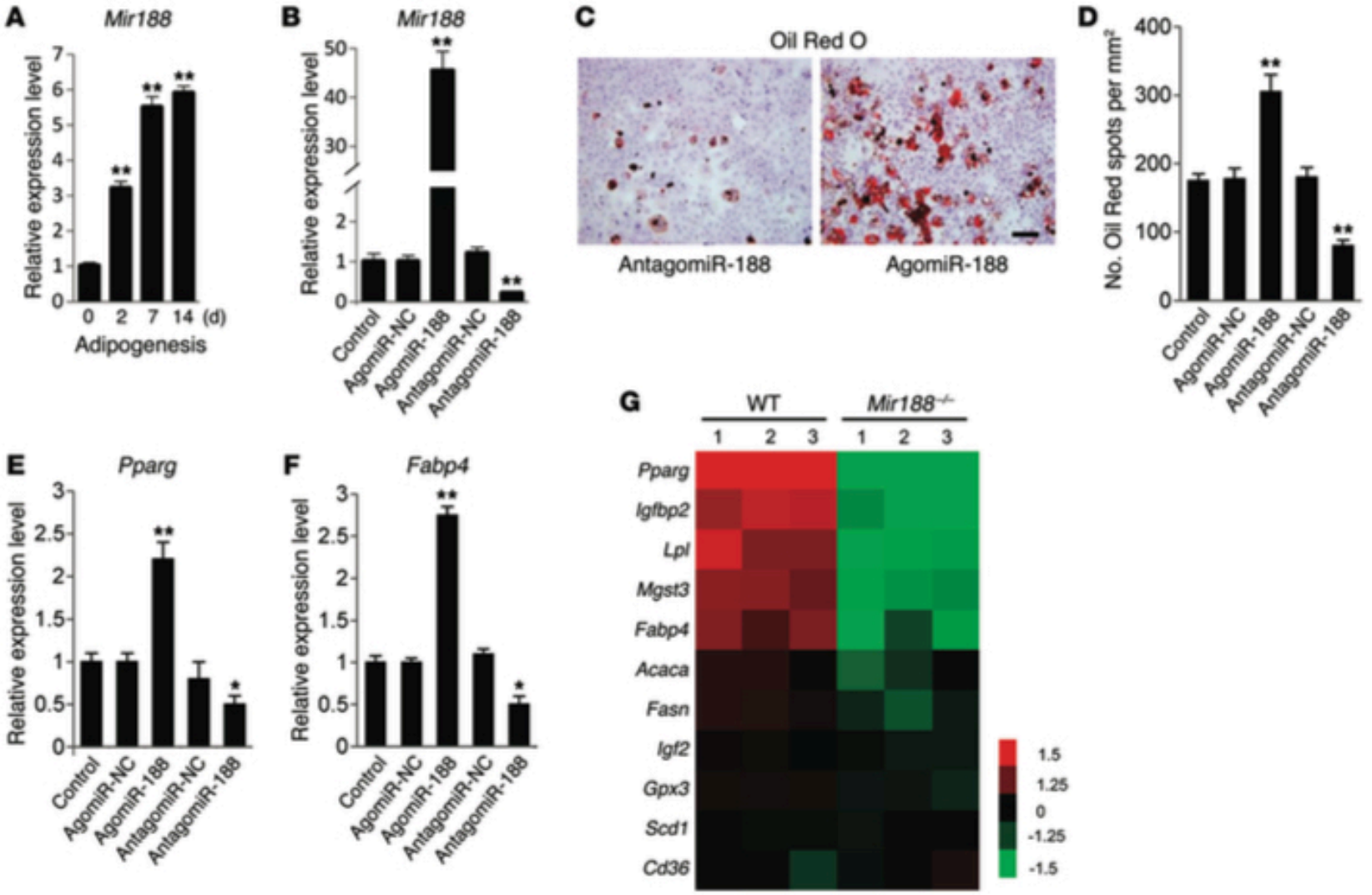

Figure 6. MiR-188 promotes adipogenic differentiation of BMSCs. (**A**) qRT-PCR analysis of the relative levels of miR-188 expression in BMSCs cultured in adipogenesis induction medium (0.5 mM 3-isobutyl-1-methylxanthine, 5 μg/ml insulin, and 1 μM dexamethasone) for the days as indicated. $n = 5$ per group. (**B**) qRT-PCR analysis of the relative levels of miR-188 expression in BMSCs transfected with 10 μM agomiR-188, antagomiR-188, or their negative controls. NC, negative control. $n = 5$ per group. (**C** and **D**) Representative images of Oil Red O staining of lipids (**C**) and quantification of the number of spots (**D**) in BMSCs cultured in adipogenesis induction medium for 14 days. Scale bar: 100 μm. (**E** and **F**) qRT-PCR analysis of the relative levels of *Pparg* (**E**) and *Fabp4* (**F**) mRNA expression in BMSCs cultured in adipogenesis induction medium for 48 hours. (**G**) Microarray profiling results of dysregulated adipogenic genes in WT and *Mir188*$^{-/-}$ mouse–derived BMSCs cultured in adipogenesis induction medium for 48 hours. Data shown as mean ± SD. $^{*}P < 0.05$, $^{**}P < 0.01$ (ANOVA).

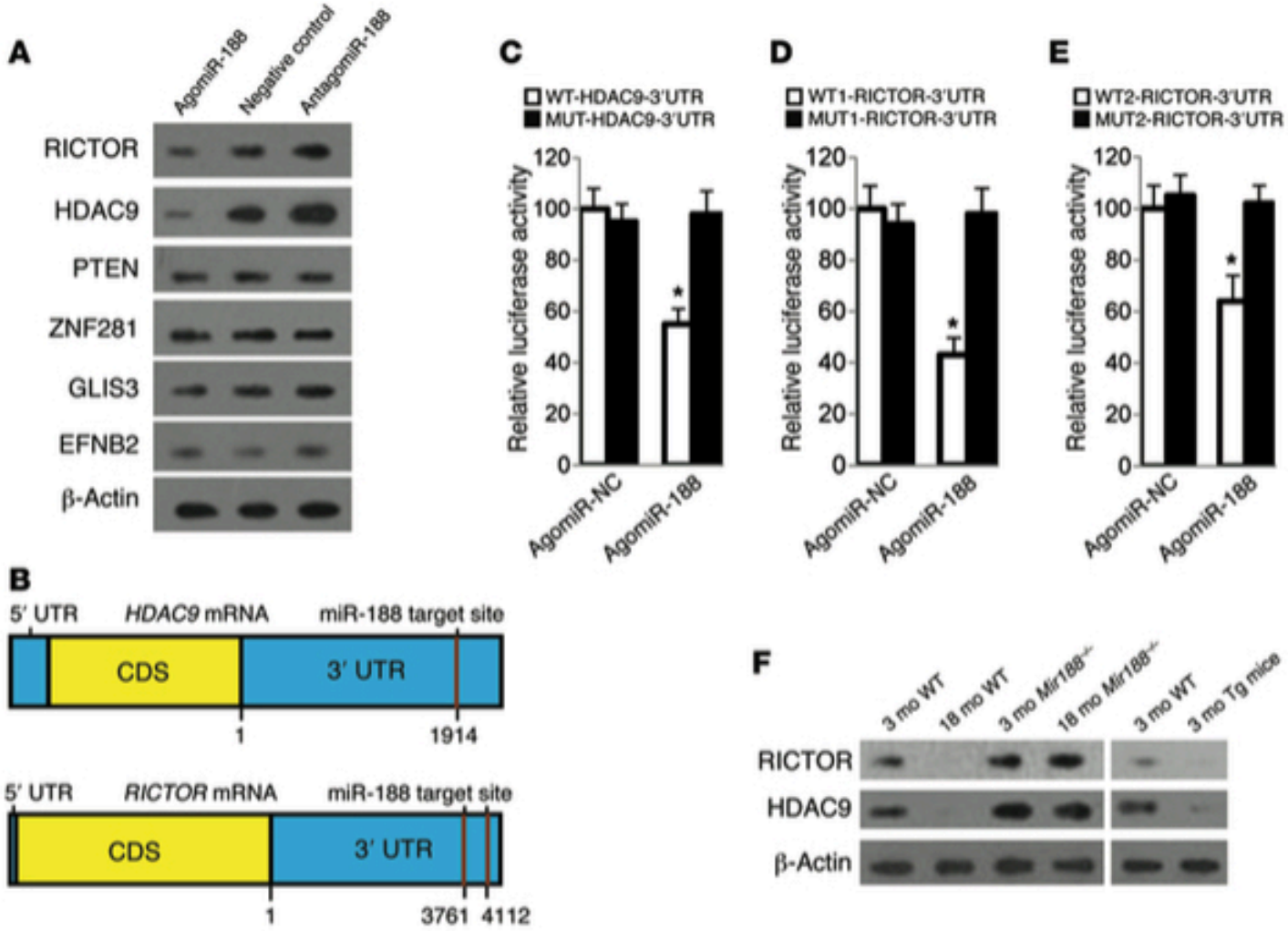

Figure 8. MiR-188 directly targets HDAC9 and RICTOR. (**A**) Western blot analysis of the relative levels of HDAC9, RICTOR, PTEN, ZNF281, GLIS3, and EFNB2 protein expression in BMSCs transfected with agomiR-188 and antagomiR-188. β-Actin was used as loading control. Data are representative of 3 independent experiments. (**B**) Schematic of miR-188 putative target sites in mouse *Hdac9* and *Rictor* 3′-UTR. CDS, coding sequence. (**C**–**E**) BMSCs were transfected with luciferase reporter carrying WT or MUT 3′-UTR of the *HDAC9* gene (WT–HDAC9–3′-UTR and MUT–HDAC9-3′–UTR) (**C**) WT1–Rictor–3′-UTR and MUT1–Rictor–3′-UTR (**D**), WT2–Rictor–3′-UTR and MUT2–Rictor–3′-UTR (**E**), respectively, and cotransfected with agomiR-188 or agomiR-NC. Effects of miR-188 on the reporter constructs were determined at 48 hours after transfection. Firefly luciferase values, normalized for renilla luciferase, are presented. $n = 3$ per group. (**F**) Western blot analysis of HDAC9 and RICTOR protein expression in BMSCs from different mice as indicated. Data are representative of 3 independent experiments. Data shown as mean ± SD. *$P < 0.01$ vs. MUT-pGL3-HDAC9 or -RICTOR (Student's *t* test).

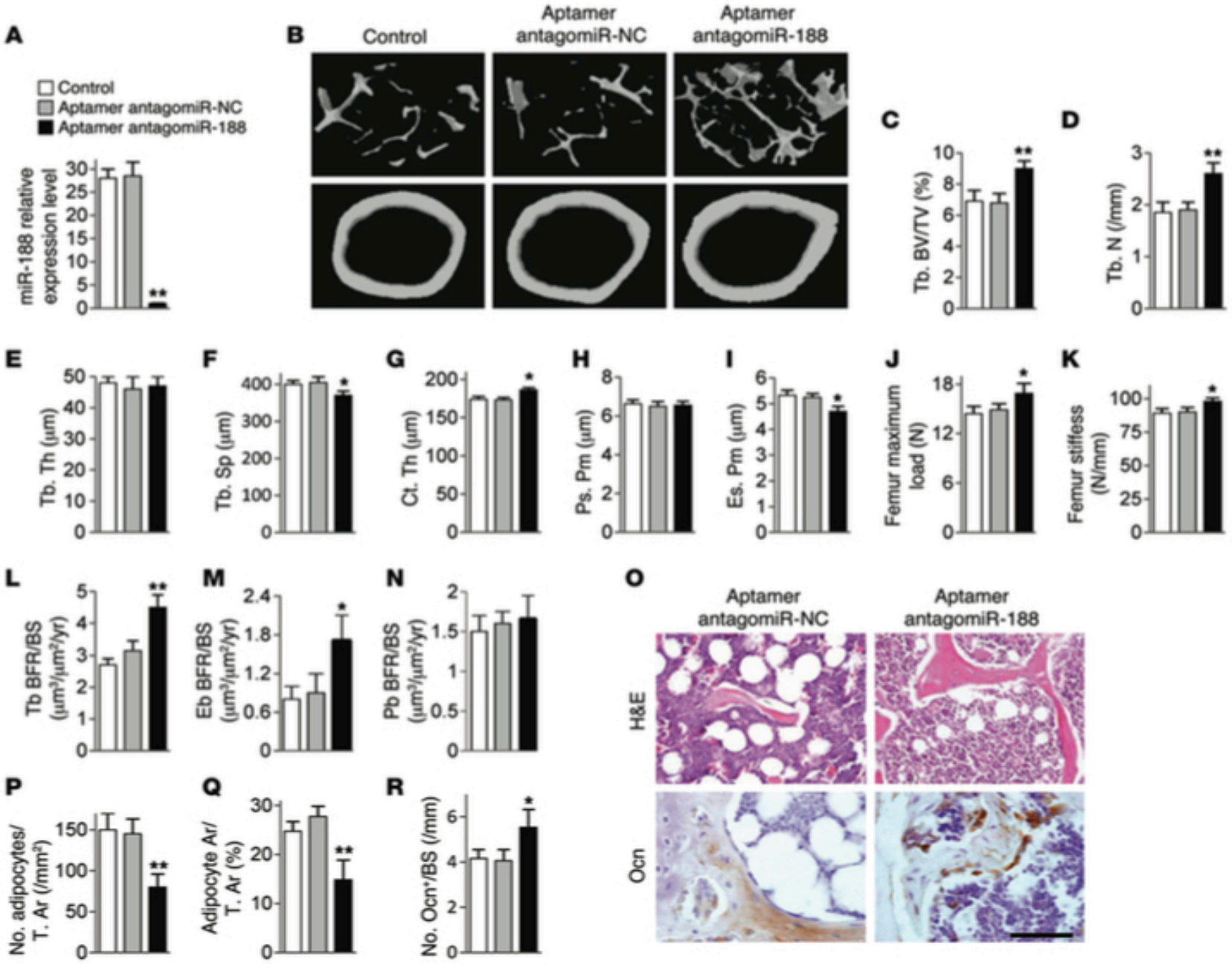

Figure 9. Injection of aptamer-antagomiR-188 into bone marrow stimulates bone formation and decreases marrow fat accumulation in aged mice. (**A**) qRT-PCR analysis of the levels of miR-188 expression in BMSCs of mice with BMSC-specific antagomiR-188 delivery. Aptamer-antagomiR-188 was injected into femoral bone marrow cavity of 15-month-old mice twice per month for 3 months. NC, negative control. (**B–I**) Representative μCT images (**B**) and quantitative μCT analysis of trabecular (**C–F**) and cortical (**G–I**) bone microarchitecture in femora from aptamer-treated mice. $n = 10$ per group. (**J** and **K**) Three-point bending measurement of femur maximum load (**J**) and stiffness (**K**). $n = 5$ per group. (**L–N**) Calcein double labeling–based quantification of

Environmental Factors
(mechanical stress
Cytokines, UVs)

intrinsec Factors
(oxidative stress-
DNA repair defects)

DNA Damage

Epigenetic changes

Changes in gene expression

Cellular Senescence

Specific Secretome (SMS)

Tissue Aging
(loss of function)

Stem-cell Aging

Systemic Aging

Organismal aging

Adapted from Brunet A. et al, Nature 2007

ACTION à distance des microRNAs sur le vieillissement tissulaire

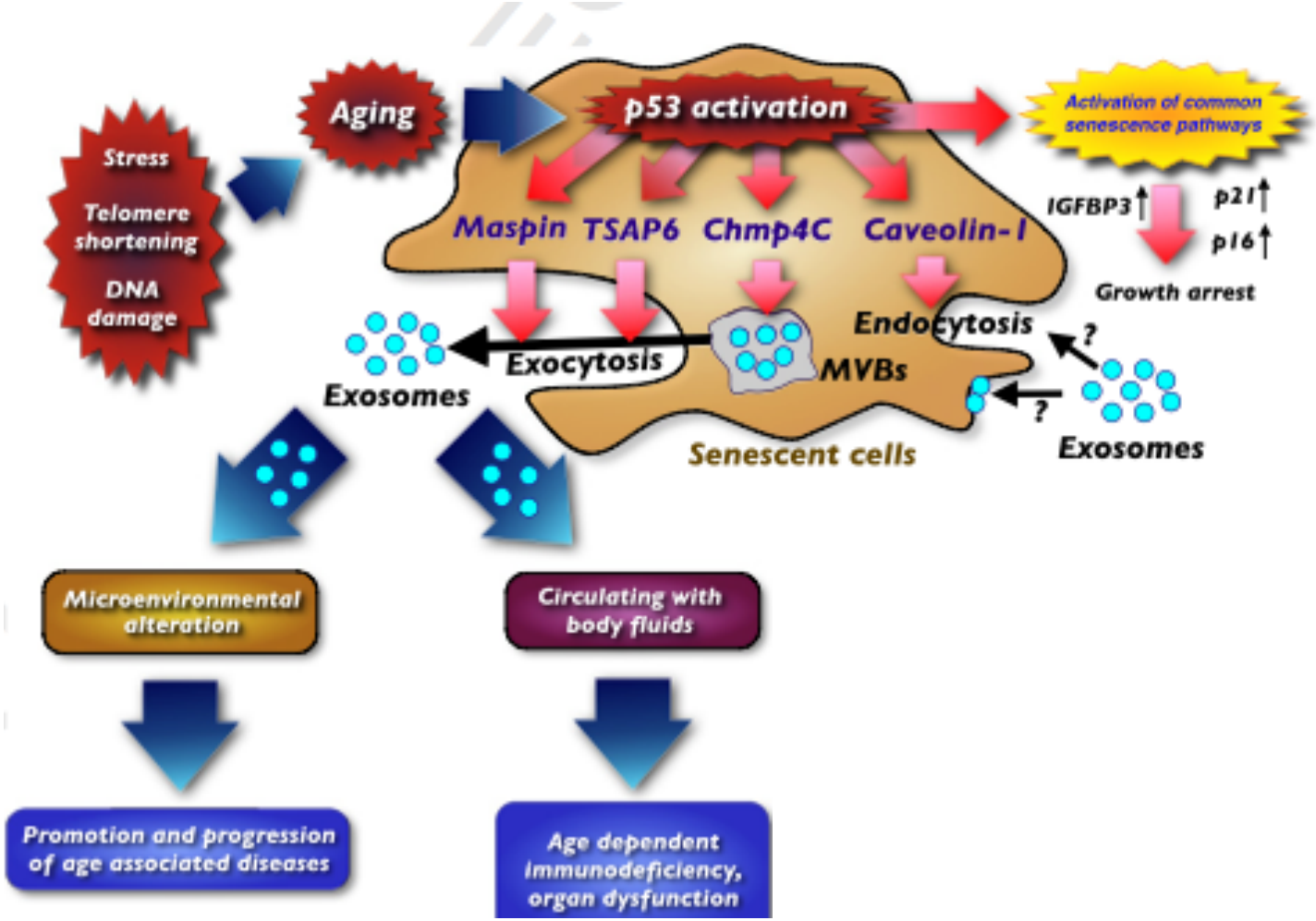

Aging Cell (2016) **15**, pp744–754 Doi: 10.1111/acel.12484

Secreted microvesicular miR-31 inhibits osteogenic differentiation of mesenchymal stem cells

Sylvia Weilner,[1,2,3,*] Elisabeth Schraml,[1,*] Matthias Wieser,[1,4] Paul Messner,[5] Karl Schneider,[1,2] Klemens Wassermann,[1,2] Lucia Micutkova,[6] Klaus Fortschegger,[7] Andrea B. Maier,[8,9] Rudi Westendorp,[10] Heinrich Resch,[11] Susanne Wolbank,[2,13] Heinz Redl,[2,13] Pidder Jansen-Dürr,[6] Peter Pietschmann,[12] Regina Grillari-Voglauer[1,3,4] and Johannes Grillari[1,3,13]

[1]Department of Biotechnology, BOKU – University of Natural Resources and

mal stem cells where it inhibits osteogenic differentiation by knocking down its target Frizzled-3. Therefore, we suggest that microvesicular miR-31 in the plasma of elderly might play a role in the pathogenesis of age-related impaired bone formation and that miR-31 might be a valuable plasma-based biomarker for aging and for a systemic environment that does not favor cell-based therapies whenever osteogenesis is a limiting factor.

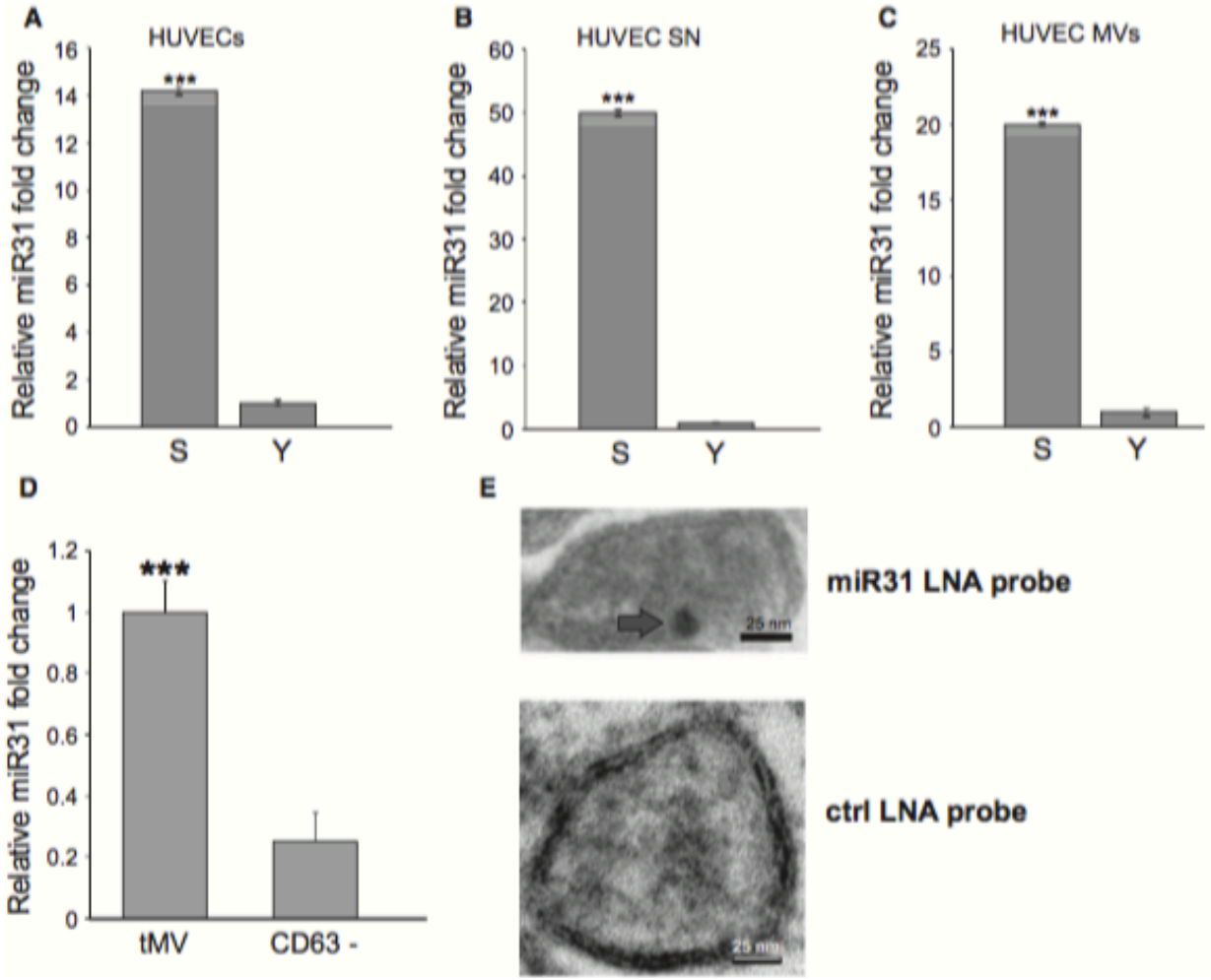

Fig. 2 miR-31 is enriched in CD63-positive microvesicles of senescent endothelial cells. (A) miR-31 expression is upregulated in senescent (S) versus early quiescent passage (Y) HUVECs ($N = 3$) as analyzed by qPCR. (B) miR-31 was detected at high levels after RNA isolation from supernatants (SN) ($N = 3$) and (C) from MVs of senescent (S) versus early quiescent (Y) passage HUVECs ($N = 3$). (D) Significantly increased miR-31 levels in tMV fraction of senescent endothelial cells compared with the $CD63^-$ fraction. (E) Localization of miR-31 within MVs. Arrowhead indicates immunogold-labeled anti-DIG antibody after hybridizing a DIG-labeled anti-miR-31 probe to permeabilized MVs. ***: $P < 0.001$ in comparison with control. Data of this figure are presented as mean values ± SD and were statistically analyzed using Student's *t*-test.

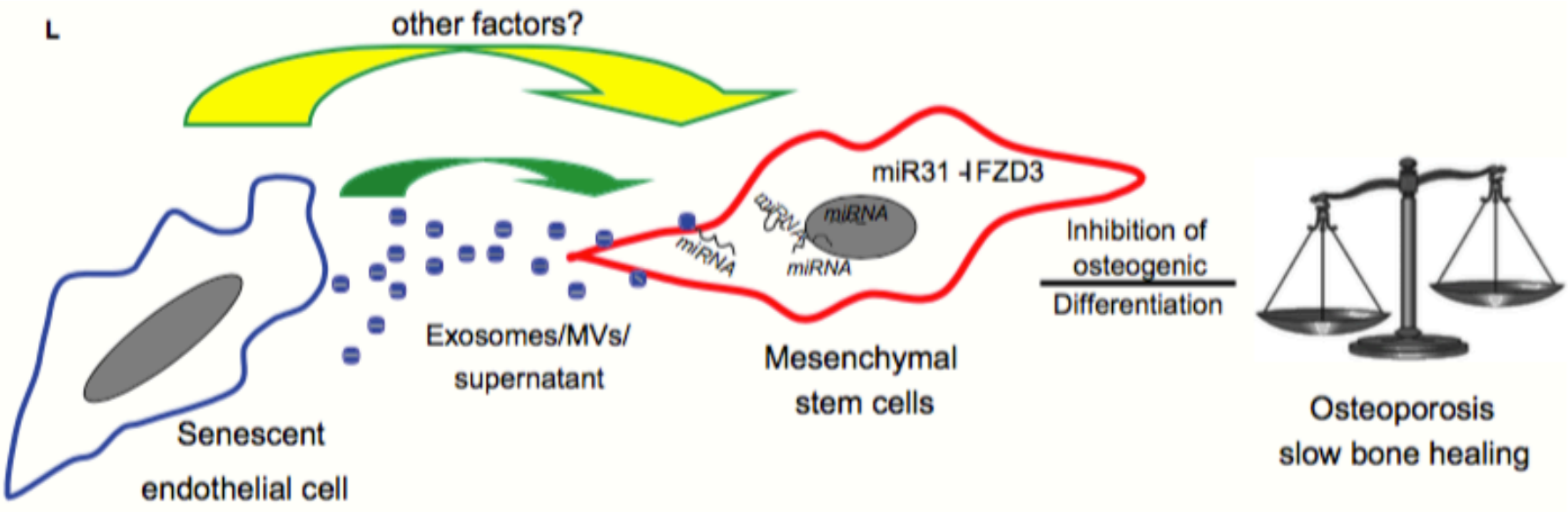
L
other factors?
miR31 -| FZD3
miRNA
miRNA
miRNA
Inhibition of
osteogenic
Differentiation
Exosomes/MVs/
supernatant
Senescent
endothelial cell
Mesenchymal
stem cells
Osteoporosis
slow bone healing

Environmental Factors
(mechanical stress
Cytokines, UVs)

intrinsec Factors
(oxidative stress-
DNA repair defects)

Cellular Senescence

DNA Damage

Epigenetic changes

Changes in gene expression

Specific Secretome (SMS)

Tissue Aging
(loss of function)

Stem-cell Aging

Systemic Aging

Organismal aging

Adapted from Brunet A. et al, Nature 2007

Current Biology 20, 2159–2168, December 21, 2010 DOI 10.1016/j.cub.2010.11.015

Article

MicroRNAs Both Promote and Antagonize Longevity in *C. elegans*

Alexandre de Lencastre,[1] Zachary Pincus,[1] Katherine Zhou,[1] Masaomi Kato,[1] Siu Sylvia Lee,[2] and Frank J. Slack[1,*]
[1]Department of Molecular, Cellular and Developmental Biology, Yale University, New Haven, CT 06511 USA
[2]Department of Molecular Biology and Genetics, Cornell University, Ithaca, NY 14850, USA

metabolism, immunity, life span, and cancer [3]—and target predictions suggest that they may regulate thousands of human genes [4]. Still, only a small number of the thousands of known miRNAs have been implicated in a specific biological function, whereas the role of the vast majority of miRNAs remains unknown. Mutations in the developmental timing genes *lin-4* (a founding member of the miRNA family) and its

Utilisation de C.elegans, un nématode

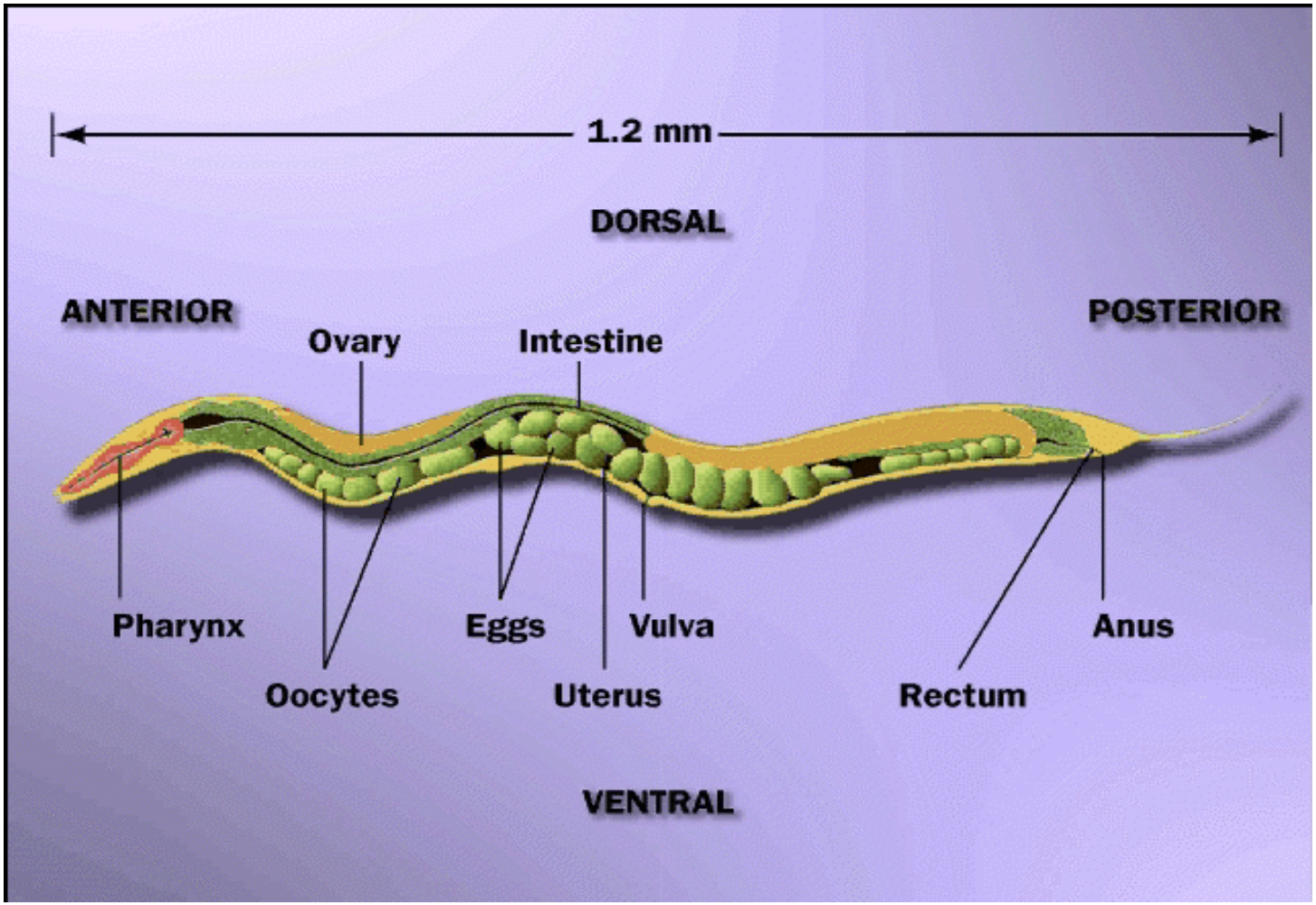

Cycle de vie de C. elegans

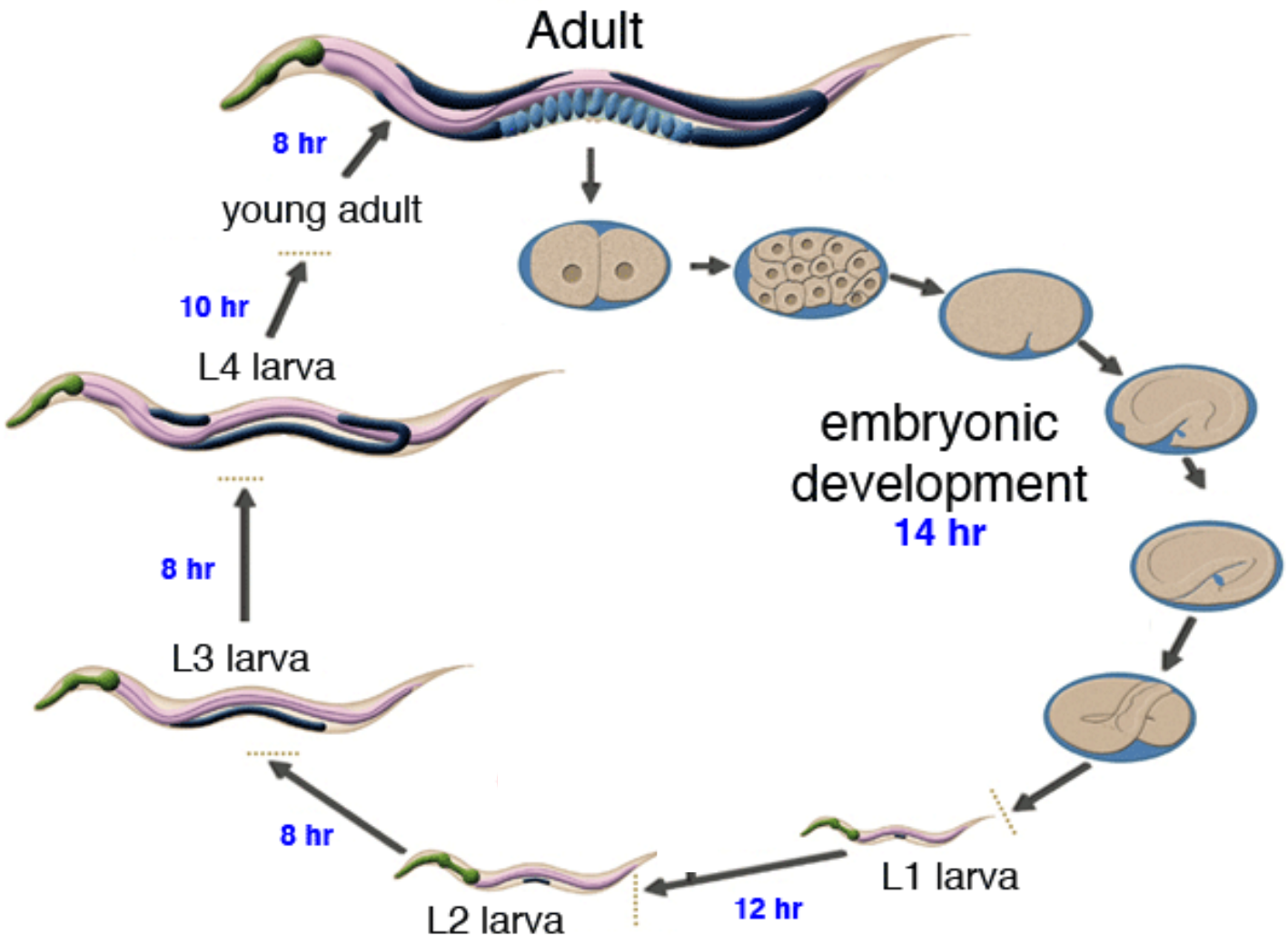

Identification et caractérisation de mutants de C. elegans

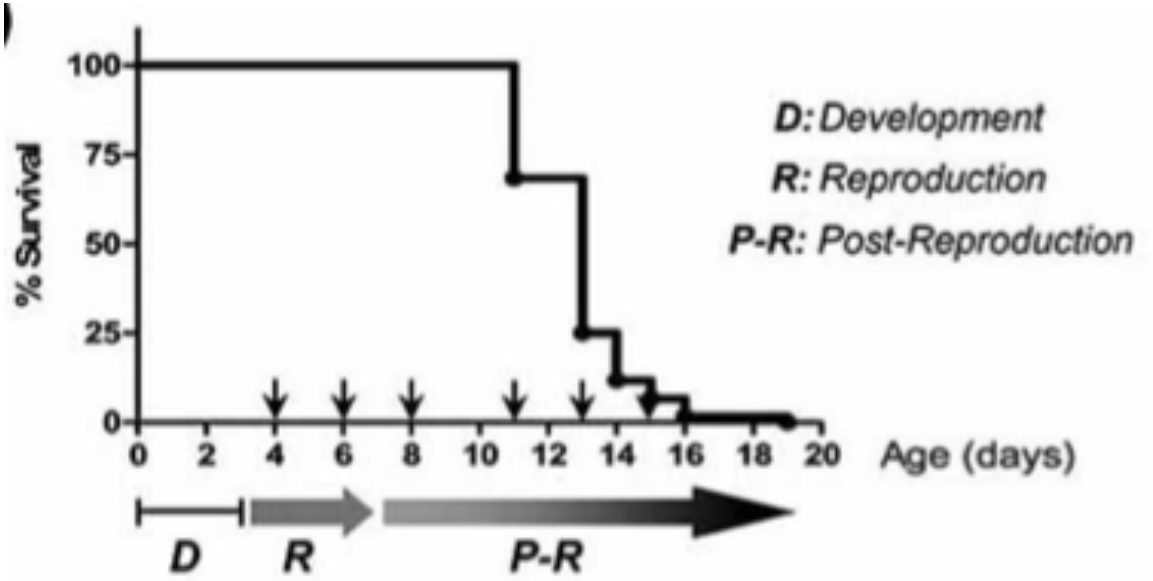

(Spe-9)

Table 1. Summary of Largest Expression Changes of miRNAs with Aging

miRNA	N2	*daf-2(e1370)*	Homology
Most Upregulated with Aging			
miR-246	*5.90*	*9.46*	
miR-71	*4.04*	*4.21*	
miR-34	*3.93*	*3.28*	miR-34
miR-253	*3.31*	1.44	miR-220
miR-238	*2.88*	*2.43*	miR-12
miR-239b	*2.85*	*6.37*	miR-12
miR-239a	*2.15*	1.91	miR-12
Most Downregulated with Aging			
let-7	*−7.38*	*−5.39*	let-7
miR-41	*−6.78*	*−2.34*	
miR-70	*−5.70*	*−3.80*	
miR-252	*−5.02*	*−2.22*	
miR-62	*−4.30*	*−2.91*	
miR-36	*−4.10*	*−2.62*	
miR-59	*−3.56*	−1.41	
miR-1829b	*−3.44*	*−2.31*	
miR-236	*−3.20*	*−3.69*	miR-200b
miR-37	*−3.20*	*−2.15*	
miR-237	*−3.14*	*−5.70*	lin-4, miR-125
miR-793	*−2.95*	*−2.13*	
miR-43	*−2.72*	*−2.10*	
miR-65	*−2.65*	−1.76	
miR-40	*−2.59*	*−2.50*	
miR-77	*−2.27*	−1.48	
miR-79	*−2.22*	*−4.93*	miR-9
miR-81	*−2.18*	−1.88	
miR-82	*−2.17*	−1.82	
miR-259	*−2.16*	−1.37	
miR-38	*−2.14*	−1.84	
miR-64	*−2.11*	−1.61	
miR-35	*−2.06*	−1.81	
miRNA	Day 0	miRNA	Day 10
Most Upregulated in *daf-2(e1370)*			
miR-237	*2.94*	miR-62	*3.00*
miR-49	*2.26*	miR-49	*2.93*
miR-253	*2.21*	miR-252	*2.22*
miR-44	*2.05*	miR-231	*2.19*
miR-45	*2.05*		
miR-62	*2.03*		
Most Downregulated in *daf-2(e1370)*			
miR-1829c	*−4.49*	miR-242	*−2.24*
miR-239b	*−3.40*		
miR-259	*−2.80*		
miR-246	*−2.04*		
miR-85	*−2.00*		

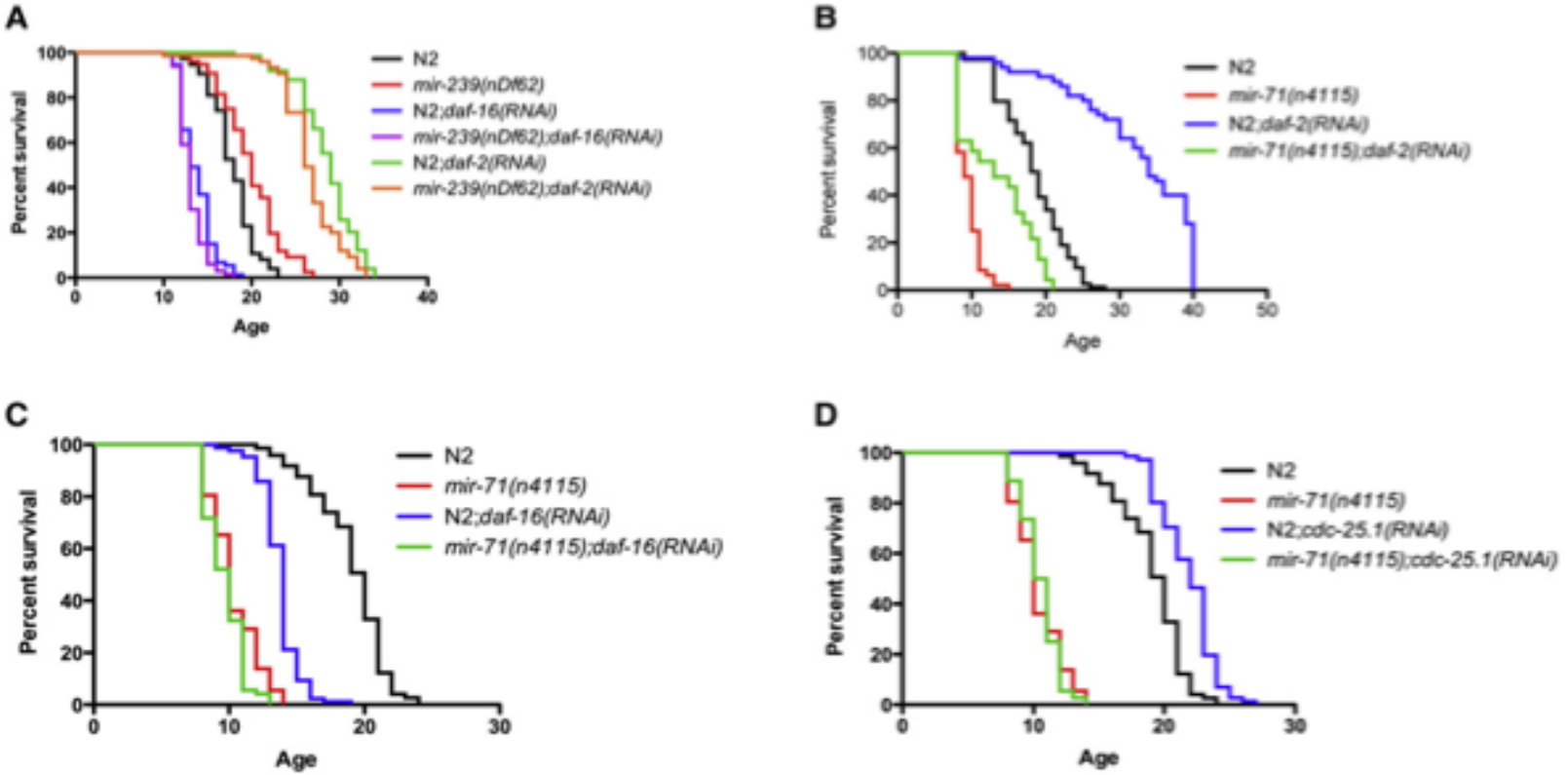

Figure 5. miR-239 and miR-71 Function through the IGF-1/Insulin-like and the DNA Damage Checkpoint Pathways

(A) The long life span of *mir-239(nDf62)* is suppressed by *daf-16(RNAi)* but is unaffected by control (empty vector) RNAi. *mir-239(nDf62)* does not further enhance life span on *daf-2(RNAi)*, suggesting that they function in the same pathway.

(B and C) The long life span of *daf-2(RNAi)* is partially suppressed by *mir-71(n4115)*, and *daf-16(RNAi)* does not further decrease the life span of *mir-71 (n4115)*, suggesting that miR-71 functions in the same pathway as DAF-2 and DAF-16.

(D) miR-71 additionally functions in the DNA damage checkpoint pathway. *mir-71(n4115)* fully suppresses the longevity induced by RNAi against CDC-25.1, a factor of the DNA damage checkpoint pathway.

All life-span assays were conducted at 20°C. Statistics are shown in Table S5.

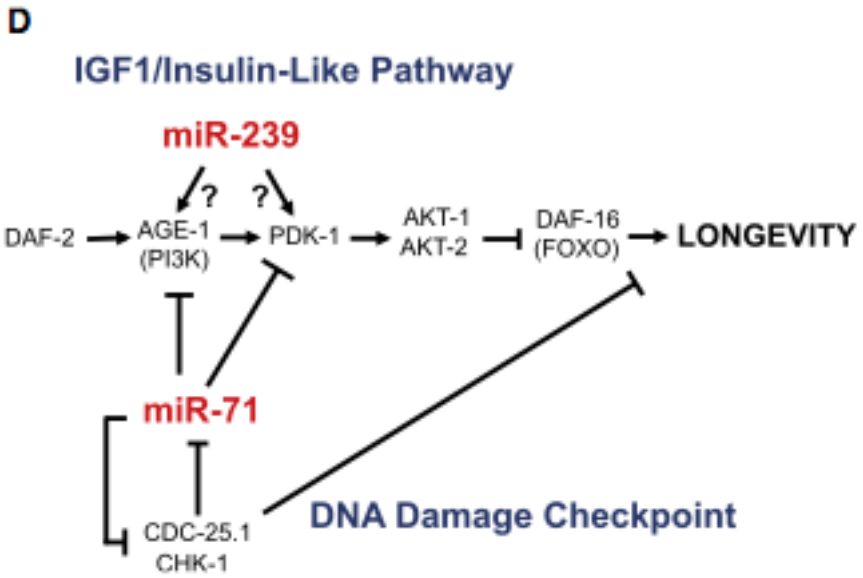
D
IGF1/Insulin-Like Pathway
miR-239
?
?
DAF-2
AGE-1
(PI3K)
PDK-1
AKT-1
AKT-2
DAF-16
(FOXO)
LONGEVITY
miR-71
CDC-25.1
CHK-1
DNA Damage Checkpoint

CONCLUSIONS:

1- Les miRs sont comme des régions codantes soumis à un contrôle épigenetique

2- Conservation des séquences des miRs inter-especes (pression de sélection/ évolution)
62% similaires entre C.elegans et la drosophile
55% similaires entre C.elegans et humain

3- Beaucoup de travail sur l'identification des cibles des miRs et de leur véritable mode d'action

4- identification de miRs régulant chez les mammifères le vieillissement général?

5- en particulier des miRs régulant en systémique le vieillissement tissulaire

Acknowledgments

Didier Philipot
David Guérit
Dr Paul Chuchana
Dr Farida Djouad
Dr Danièle Noël
Pr Christian Jorgensen
INSERM U1183

Dr Charles Lecellier
Dr Jacques Piette

SERVIZIO SANITARIO REGIONALE
EMILIA - ROMAGNA
Istituto Ortopedico Rizzoli di Bologna
Istituto di Ricovero e Cura a Carattere Scientifico

Dr Rosa Maria Borzi
Dr Eleonora Olivotto
Dr Daniela Platano

CHRU MONTPELLIER
CENTRE HOSPITALIER REGIONAL UNIVERSITAIRE

Immuno-rhumatologie et thérapeutique des maladies osseuses et articulaires

www.irmb.com

Montpellier Aging Network